pmod wrc

Annual Report 2010
Jahresbericht 2010

Physikalisch-Meteorologisches Observatorium Davos und Weltstrahlungszentrum

Mission

Das PMOD/WRC

- dient als internationales Kalibrierzentrum für meteorologische Strahlungsmessinstrumente;
- entwickelt Strahlungsmessinstrumente für den Einsatz am Boden und im Weltraum;
- erforscht den Einfluss der Sonnenstrahlung auf das Erdklima.

Auftragerteilung

Das Physikalisch-Meteorologische Observatorium Davos (PMOD) beschäftigt sich seit seiner Gründung im Jahr 1907 mit Fragen des Einflusses der Sonnenstrahlung auf das Erdklima. Das Observatorium schloss sich 1926 dem Schweizerischen Forschungsinstitut für Hochgebirgsklima und Medizin Davos an und ist seither eine Abteilung dieser Stiftung. Auf Ersuchen der Weltmeteorologischen Organisation (WMO) beschloss der Bundesrat im Jahr 1970 die Finanzierung eines Kalibrierzentrums für Strahlungsmessung als Beitrag der Schweiz zum Weltwetterwacht-Programm der WMO. Nach diesem Beschluss wurde das PMOD beauftragt, das Weltstrahlungszentrum (World Radiation Center, WRC) zu errichten und zu betreiben.

Kerntätigkeiten

Das Weltstrahlungszentrum unterhält das Primärnormal für solare Bestrahlungsstärke bestehend aus einer Gruppe von hochpräzisen Absolut-Radiometern. Auf weitere Anfragen der WMO wurden 2004 das Kalibrierzentrum für Messinstrumente der atmosphärischen Langwellenstrahlung eingerichtet und 2008 das Kalibrierzentrum für spektrale Strahlungsmessungen zur Bestimmung der atmosphärischen Trübung. Seit 2007 wird auch das Europäische UV Kalibrierzentrum durch das Weltstrahlungszentrum betrieben. Das Weltstrahlungszentrum besteht heute aus vier Sektionen:

- Solare Radiometrie
- Infrarot Radiometrie
- Atmosphärische Trübungsmessungen (WORCC)
- Europäisches UV Kalibrierzentrum

Die Kalibriertätigkeit ist in ein international anerkanntes Qualitätssystem eingebettet (ISO 17025) um eine zuverlässige und nachvollziehbare Einhaltung des Qualitätsstandards zu gewährleisten.

Das PMOD/WRC entwickelt und baut Radiometer, die zu den weltweit genauesten ihrer Art gehören und sowohl am Boden als auch im Weltraum eingesetzt werden. Diese Instrumente werden auch zum Kauf angeboten und kommen seit langem bei Meteorologischen Diensten weltweit zum Einsatz. Ein globales Netzwerk von Stationen zur Überwachung der atmosphärischen Trübung ist mit vom Institut entwickelten Präzisionsfilterradiometern ausgerüstet.

Im Weltraum und mittels Bodenmessungen gewonnene Daten werden in Forschungsprojekten zum Klimawandel und der Sonnenphysik analysiert. Diese Forschungstätigkeit ist in nationale, insbesondere mit der ETH Zürich, und internationale Zusammenarbeit eingebunden.

Das PMOD/WRC ist eine Abteilung der Stiftung
Schweizerisches Forschungsinstitut für
Hochgebirksklima und Medizin in Davos.

Physikalisch-Meteorologisches Observatorium Davos
und World Radiation Center (PMOD/WRC)
Dorfstrasse 33
7260 Davos Dorf
Schweiz

pmod wrc

Annual Report
Jahresbericht 2010

Annual Report 2010

Table of Contents

Jahresbericht 2010

Werner Schmutz

Dienstleistungsbetrieb Weltstrahlungszentrum

Pyrheliometer sind meteorologische Strahlungsmessgeräte, die die direkte Bestrahlungsstärke der Sonne messen. Die Resolution 13 des Executive Council der WMO verlangt, dass alle fünf Jahre Internationale und Regionale Pyrheliometer-Vergleiche durchgeführt werden. Diese Vergleiche sind dazu da, die Qualität der weltweit verteilten operationellen Standard-Instrumente im direkten Vergleich mit der Weltstandardgruppe zu überprüfen. Am 9. März 2010 hat die WMO die interessierten Kalibrierzentren zur Teilnahme an den Elften Pyrheliometer Vergleichen (IPC-XI) aufgefordert. Diese fanden vom 27. September bis zum 15. Oktober 2010 unter ausgezeichneten Wetterbedingungen am Weltstrahlungszentrum in Davos statt. Wie bereits während der vergangenen zwei IPCs wurden zeitgleich auch Filterradiometer-Vergleiche (zur Trübungsbestimmung) durchgeführt. Dieses Mal fanden zudem erstmals Pyrgeometer-Vergleiche statt. Pyrgeometer sind Strahlungsgsinstrumente, die zur Messung der infraroten Strahlung eingesetzt werden. Ein wesentlicher Teil der Mitarbeitenden war schon viele Monate vor den IPC-XI mit Vorbereitungsarbeiten beschäftigt. In den Monaten September und Oktober aber, war praktisch jedermann/jedefrau ununterbrochen in die Organisation des Anlasses involviert. Ich kann stolz berichten, dass der engagierte Einsatz der Mitarbeitenden reibungslose und sehr erfolgreiche Vergleiche ermöglicht hat. Ich benutze daher diese Gelegenheit, meinen Mitarbeiterinnen und Mitarbeitern meine volle Anerkennung für ihren Einsatz und ihre harte Arbeit auszusprechen und ihnen herzlich dafür zu danken.

Ergänzend und passend zum operationellen Erfolg der IPC-XI ist der Abschluss einer formellen Übereinkunft zwischen der WMO und dem PMOD/WRC. Mit Vertrag vom 1. April 2010 überträgt die Meteorologische Weltorganisation dem Weltstrahlungszentrum die Vertretung bei der Internationalen Organisation für Masse und Gewichte. Dies gilt als Beitritt zum gegenseitigen Anerkennungsabkommen der Metrologischen Institute (CIPM-MRA) für die Messgrösse Solare Bestrahlungsstärke. Nur drei Wochen später, am 20. April 2010, wurde ein ähnlicher Vertrag zwischen dem Bundesamt für Metrologie (METAS) und dem PMOD/WRC unterzeichnet. Dieser Vertrag war die formelle Bestätigung des Weltstrahlungszentrums als designiertes Institut des METAS für Solare Bestrahlungsstärke beim CIPM-MRA.

Entwicklung und Bau von Experimenten

Die Entwicklung des kryogenen Radiometers CSAR (Cryogenic Solar Absolute Radiometer) spielt eine zentrale Rolle für die Zukunft des Weltstrahlungszentrums. Dieses Projekt ist eine Zusammenarbeit mit den Metrologie-Instituten National Physics Laboratory in England und dem METAS in Bern. Während der IPC-XI wurde CSAR zum ersten Mal eingesetzt und kleinere Mängel wurden anschliessend eliminiert. Das Instrument misst nun hervorragend und wir erwarten, dass das Ziel, die solare Bestrahlungsstärke um einen Faktor zehn genauer messen zu können, erreicht werden kann. Das bedeutet, dass mit der Zeit von der bisherigen, auf einer Gruppe von Instrumenten basierenden Referenz, auf eine Realisierung der Messgrösse gewechselt werden kann, die auf das Internationale Einheitssystem rückführbar ist. Die Installation von CSAR am Weltstrahlungszentrum ist die Gewähr dafür, dass wir auch in Zukunft eine führende Rolle in der Kalibrierung von Strahlungsmessinstrumenten behalten können.

Weltraumprojekte

Am 15. Juni 2010 wurde die Französische Mission PICARD mit vier Experimenten gestartet; eines davon ist das Experiment PREMOS, das am Observatorium gebaut wurde. Das PREMOS Experiment besteht aus zwei Absolut-Radiometern des Typs PMO6 und drei Vier-Kanal-Filterradiometern. Eines der Absolutradiometer ist das erste Instrument im Weltraum das lückenlos auf das Internationale Einheitssystem rückführbar kalibriert ist. Am 27. Juli 2010 wurde mit dem kalibrierten Absolut-Radiometer zum ersten Mal die Sonnenstrahlung gemessen. Die sorgfältige Analyse dieser ersten Messungen ergab einen Wert von 1361 W/m^2 für die Solarkonstante. Dieser Wert stimmt ausgezeichnet mit dem Wert überein, der vom Amerikanischen Experiment TIM auf dem Satelliten SORCE gemessen wird, das seit sieben Jahren im Weltraum operationell ist. Damit ist nun bestätigt, dass die Solarkonstante tatsächlich rund 4 W/m^2 kleiner ist, als drei weitere langjährige, aktive Weltraumexperimente es angeben. Seit der rund 10 Mal grössere Unterschied als die vermeintliche Messunsicherheit bekannt ist, wurde gerätselt, welcher Wert wohl richtig sei.

Über den Start der ESA Technologie Mission PROBA2 am 2. November 2009 mit dem am PMOD/WRC gebauten Instrument LYRA wurde schon im letzten Jahresbericht berichtet. Nach der Inbetriebnahme von LYRA im Januar 2010 wurden umfangreiche Tests durchgeführt, die vom Instrument erfolgreich bestanden wurden, und seitdem beobachtet LYRA im vorgesehenen Dauerbetrieb die solare Strahlung im ultravioletten Wellenlängenbereich. Die automatische Verarbeitung der rohen Messwerte zu kalibrierten Strahlungswerten ist Aufgabe des Teams am Königlich-Belgischen Observatorium. Diese Daten können nun in Fast-Echtzeit von einer interessierten Forschergemeinschaft zur Beurteilung des Weltraumwetters abgerufen werden. Ein Französisches Forschungsteam rekonstruiert für jeden Tag aus den LYRA Daten und weiteren Sonnenbeobachtungen das ganze Sonnenspektrum. Dieses rekonstruierte Sonnenspektrum wiederum wird am PMOD/WRC im Rahmen des FP7 Projektes SOTERIA zur Berechnung der chemischen Zusammensetzung der Mittleren Atmosphäre benutzt. Die ganze Kette bis zur Erstellung unseres „Now-cast“ läuft noch nicht völlig reibungslos, aber die entsprechende Webseite ist bereit und wird im ersten Forschungsbeitrag in diesem Jahresbericht vorgestellt.

Klimaforschung

Im September 2010 startete eine Kollaboration von Schweizer Forschungsinstituten ein neues Projekt namens Future and Past Solar Influence on the Terrestrial Climate (FUPSOL). Das Drei-Jahresprojekt ist ein vom Schweizerischen Nationalfonds gefördertes Sinergia-Verbundprojekt und unterstützt insgesamt fünf Vollzeit Forscherstellen und eine 50 % Stelle für

die Projektführung. Die Partner des PMOD/WRC sind das Institut für Atmosphären- und Klimawissenschaften der ETH Zürich, die Eidgenössische Anstalt für Wasserversorgung, Abwasserreinigung und Gewässerschutz (EAWAG), das Physikalische Institut der Universität Bern und das Oeschger Zentrum der Universität Bern. Wie der Titel des Projekts zum Ausdruck bringt, ist es das Ziel der Forschung, den vergangenen, wie auch einen möglichen zukünftigen Einfluss der Sonne auf das Klima zu quantifizieren.

Die vielen Beiträge der Klimagruppe in diesem Bericht sprechen für ihre vielseitigen Aktivitäten und die hohe Produktivität. Wie oben im Rahmen des FUPSOL Projekts erwähnt, ist eines unserer zentralen Ziele, den Einfluss der Sonne auf frühere Klimavariationen zu verstehen. Diese Klimarechnungen brauchen u. a. die Rekonstruktion der zeitlichen Entwicklung der Sonneneinstrahlung als eine der bestimmenden Einflüsse. In einem Beitrag von Shapiro et al. berichten wir von einem neuen Ansatz der eine starke historische Variation der solaren Strahlung ergibt. Das FUPSOL Projekt wird die Konsequenzen eines starken Sonneneinflusses ausloten.

Personelles

Fünf Mitarbeiter kamen neu an das PMOD/WRC und fünf verliessen uns und damit blieb die Zahl der Mitarbeiter gleich bei 36. Die Zahl der Doktoranden per Ende 2010 blieb mit Sechs auch konstant, obwohl es vier Mutationen gab. Stefan Wacker verteidigte im Dezember seine Dissertation erfolgreich und arbeitet nun als promovierter Forscher weiterhin am Observatorium. Ich gratuliere ihm herzlich zu seinem erfolgreichen Abschluss. Uwe Schlifkowitz hat uns verlassen und zwei Doktoranden haben neu bei uns angefangen, Edgar Schmucki und Markus Suter.

Samuel Prochazka hat seine Lehre abgeschlossen und wir gratulieren ihm zu seinem erfolgreichen Abschluss als Elektroniker. Für ihn kam Thierry Hartmann zu uns in die Lehre. Zur Unterstützung unserer Administration haben wir Irene Keller eingestellt. Unser Gastwissenschaftler vom NOAA, Pieter Kiedron, der sich in der ersten Phase bei der Neuentwicklung eines Spektroradiometers um den Instrumenten-Design gekümmert hatte, kehrte im Januar 2011 wieder nach Boulder, USA zurück. An seiner Stelle ist Etienne de Coulon eingestellt worden, der als Ingenieur die Realisation des Prototyp-Instruments unterstützt.

Mit der Renovation des Hauses haben wir die im Hause liegende Abwartswohnung verloren. Dies hatte zur Folge, dass unsere bisherigen Abwartsfrauen, Denise Dicht und Jutta Jäger ihre Stelle aufgegeben haben. Neu kümmert sich nun Stana Petrovic um unser Wohlergehen in einem schwierigen Umfeld zwischen provisorischen Arbeitsplätzen in den Containern und dem laufendem Umbau im Haus.

Die wichtigste personelle Änderung betrifft Silvio Koller, der uns nach acht Jahren am Observatorium verlassen hat. Er war ursprünglich für das Weltraumprojekt LYRA verantwortlich und ab 2008 der Leiter der technischen Abteilung und damit auch Mitglied der Institutsleitung. Unter seiner kompetenten Leitung konnten wir die Vielzahl unserer kleinen und grossen Projekte zu einem erfolgreichen Abschluss bringen. Wir danken ihm herzlich für seinen engagierten Einsatz und wertvollen Beitrag zum Erfolg des PMOD/WRC. Er ist nun Geschäftsführer einer Firma für Solarenergietechnik und wir wünschen ihm bei seiner neuen Tätigkeit alles Gute und viel Erfolg. Der neue Leiter der technischen Abteilung ist Manfred Gyo, der Anfang 2011 ans Observatorium gekommen ist.

Infrastruktur

Die im Jahr 2009 gebauten Nottreppe und Lift auf der Westseite des Alten Schulhauses wurden im Frühjahr 2010 fertig gestellt. Parallel dazu lief die Fertigstellung der Projektdefinition der Erneuerung der Infrastruktur durch das Bundesamt für Bauten und Logistik und dem beauftragten Generalplaner Emch und Berger. Die Projektdokumentation konnte im September 2010 vom Nutzer unterzeichnet werden.

Gleich nach Abschluss der IPC-XI begannen die ersten Umbauarbeiten des Alten Schulhauses. Sichtbares Zeichen für den Baubeginn ist ein Baukran, der zusammen mit der Infrastruktur der Baustelle die Hälfte des Parkplatzes einnimmt. Während etwas mehr als die Hälfte der Mitarbeiter nach Ostern 2011 in die ehemalige Holländische Klinik umziehen wird, bleibt die Technik-Abteilung auf dem Gelände. Noch Ende 2010 bezogen sie ein provisorisches zweistöckiges Gebäude, das aus neun Containern im vorderen Teil der Messwiese aufgebaut wurde. Die Messinstrumente wurden vom Dach des Alten Schulhauses entfernt auf das Dach der Container montiert. Ausgewählte Instrumente der Weltstandardgruppe bekamen dort ebenfalls einen neuen provisorischen Standort, so dass der Dienstleistungsbetrieb des Weltstrahlungszentrums auch während der Umbauphase gewährleistet ist.

Dank

Nach einem Jahr, in dem Internationale Pyrheliometer Vergleiche stattgefunden haben, gehört die wichtigste Anerkennung den Mitarbeitenden des Observatoriums für ihren engagierten Einsatz. Alle zusammen haben bei unseren internationalen Teilnehmern den positiven Eindruck hinterlassen, dass sich ein motiviertes und kompetentes Team für die Kalibrierung von Strahlungsmessinstrumenten einsetzt. Ich danke herzlich für alle Beiträge zu diesem erfolgreichen Jahr.

Im Verlauf des letzten Jahres haben die Vorgespräche für die Erneuerung der Finanzierung des Weltstrahlungszentrums stattgefunden. Wir fanden in allen Gremien Anerkennung für unsere Arbeit und Unterstützung für unser Anliegen den Vertrag zu erneuern. Ich danke allen involvierten Personen beim Bund, dem Kanton Graubünden und der Gemeinde Davos für diese positive Haltung. Dem Bund gehört ein zweites riesiges Dankeschön für die Finanzierung der Erneuerung unserer Infrastruktur.

Die Mitglieder des Ausschusses des Stiftungsrates und die Mitgliedern der Aufsichtskommission des Weltstrahlungszentrums verdienen durch ihre stete Unterstützung und Begleitung der Anliegen des PMOD/WRC grossen Dank. Ohne ihre Arbeit im Hintergrund wären die nach aussen sichtbaren Leistungen des Observatoriums nicht möglich.

Introduction

Werner Schmutz

Resolution 13 of the WMO Executive Council specifies that International and Regional Pyrheliometer Comparisons should be carried out at five-yearly intervals to check the quality of the operated radiation standards against the instruments of the World Standard Group. On March 9, 2010, WMO invited groups to participate in the Eleventh International Pyrheliometer Comparison (IPC-XI). The comparison was held from September 27 to October 15, 2010 in Davos under very favorable weather conditions. Similar to the previous two IPCs, simultaneous comparisons of filter radiometers to determine aerosol optical depth were also conducted. In addition, a comparison of pyrgeometers to measure infrared radiation took place for the first time. Many months before IPC-XI, a large fraction of the observatory's staff was involved in preparations, while almost everybody was fully occupied with organizational duties in September and October. I am very glad to say that their efforts resulted in smooth and successful comparisons. Let me take this opportunity to express my deepest appreciation to the observatory's personnel for their hard work and dedication.

Complementing the operational success of IPC-XI, there was a formal agreement between WMO and the PMOD/WRC, dated April 1, 2010, that the World Radiation Center would represent WMO in the Mutual Recognition Arrangement of the International Committee for Weights and Measures (CIPM-MRA) for the measurement quantity solar irradiance. Only three weeks later, on April 20, 2010, a similar contract was signed between the Swiss Federal Office of Metrology (METAS) and PMOD/WRC. The latter was the formal confirmation of the designation by METAS of the World Radiation Center to the CIPM-MRA that had already been made in September 2002.

Of central importance for the future of the World Radiation Center is the development of a Cryogenic Solar Absolute Radiometer (CSAR). This project is a collaboration with two metrology institutes, the National Physical Laboratory, UK and METAS, Bern. During IPC-XI, CSAR was operated for the first time. Minor shortcomings were identified and eliminated afterwards. The instrument is now performing well, and it is anticipated that the goal of improving the accuracy of solar irradiance measurements by a factor of ten can be achieved. This implies that eventually, there will be a change from an artifact based conventional primary reference to an SI traceable technological realization of the irradiance reference. The installation of CSAR at the PMOD/WRC ensures that the World Radiation Center will also maintain its leading role in irradiance calibrations in the future.

PMOD/WRC is also emphasizing its role as one of the major research institutes for measuring the solar constant in space. The in-house built space experiment PREMOS on the French satellite PICARD is the first fully SI traceable absolute radiometer in space. A careful evaluation of its first light on July 27, 2010 yielded a solar constant value of 1361 W/m^2. This value is very close to that measured by the TIM experiment on the American SORCE satellite, which has been operational in space for seven years. Thus, it has now been established, through a calibrated and traceable experiment, that the solar constant is lower by more than 4 W/m^2 than indicated by the other three space experiments that are presently still operational.

A renewal of the contract for funding the World Radiation Center in the next period from 2012 to 2015 was negotiated in the past year. A continuation would appear evident given the record number of participants at IPC-XI, and also, as in the years before, an ever increasing number of instruments that were calibrated. Indeed, all parties have announced a continuation of the contract. Thus, the financial future of the World Radiation Center appears to be on a solid base.

International Comparisons – Impressions








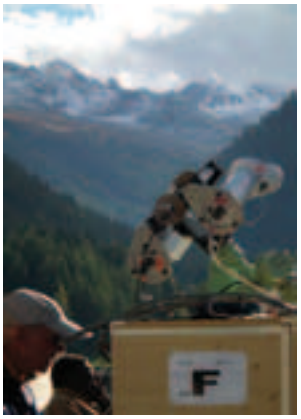



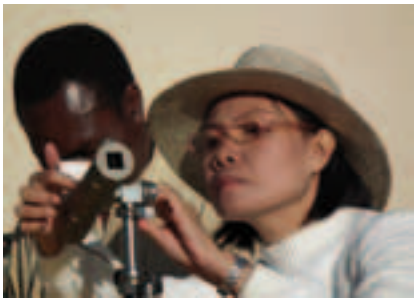



















Photos:
Diego Wasser, PMOD/WRC.

International Comparisons

XI. International Pyrheliometer Comparisons

Wolfgang Finsterle

The Eleventh International Pyrheliometer Comparisons (IPC-XI) took place at PMOD/WRC from September 27 to October 15. Eighty-seven participants from 40 countries were calibrating 99 pyrheliometers. In addition, 27 pyrheliometers including the six World Standard Group (WSG) instruments and the new Cryogenic Solar Absolute Radiometer (CSAR) were operated by PMOD staff.

Although clouds were often looming on the horizon, the sky above Davos was clear enough to take measurements on 14 days during the 3-week period. The resulting large amount of data will allow a solid evaluation and calculation of the new WRR factors for the participating instruments to be made.

The WSG continued to show signs of aging. During the course of the past five years three WSG instruments (HF18748, MK67814, and PAC3) had to be temporarily excluded from the calculation of the World Radiometric Reference (WRR). Preliminary analysis suggests that during IPC-XI only four of the six WSG instruments were stable enough to be considered for calculating the WRR. Although the WMO requirements for minimal population of the WSG are still met, the stability problems of some WSG instruments clearly emphasizes the need for replacement of the WSG by newer instruments and/or technology. The WRC currently operates several radiometers of PMO6 and AHF type which have a long-term stability record and could be integrated in the WSG in the short-term should the stability problems persist or even grow.

Unfortunately, the official WSG candidate instruments SIAR-2a and SIAR-2b were not meeting the long-term stability requirements to become members of the WSG.

On the other hand, the CSAR project, which started in 2007, made good progress (see section “Instrument Development”). CSAR adopts cryogenic technology for solar radiometry and aims at a ten-fold reduction of the absolute uncertainty as compared to ambient-temperature radiometers. This improvement would allow a re-definition of the WRR through cryogenic radiometry as opposed to the current artifact-based definition of the WRR through the WSG.

Another notable participation was by the TIM-Witness radiometer, a ground-based version of the TIM radiometer which is flying on the SORCE satellite. TIM measurements in space are systematically lower than those of WRR traceable space radiometers (such as the PMO6 on VIRGO). This first-time comparison of the TIM-Witness against the WRR will help to pin down what causes the observed differences.

On cloudy days the IPC-XI symposium and a “Course on Radiation Measurements” were held. The symposium included presentations by participants while the course was given by experts from PMOD/WRC. Of the originally planned three topics (“Instrument and Equipment Setup”, “Measurements and Calibrations”, and “Quality Management and Quality Assurance”) only the former two were given due to the limited number of cloudy days.

Figure 1. IPC-XI participants are concentrating on accurately pointing and timing their pyrheliometers. Solar irradiance levels depend strongly on atmospheric conditions. Accurate comparison of instrumental sensitivities are only possible with simultaneous irradiance measurements. Therefore scientists from all over the world gather at PMOD/WRC every five years to ensure compatibility of their solar irradiance data with the World Radiometric Reference (WRR). Photo: Ellen Røed, Norway.

First International Pyrgeometer Intercomparison

Julian Gröbner and Stefan Wacker

Taking advantage of the available synergy during IPC-XI, an intercomparison of pyrgeometers was organised between 10 participants of IPC-XI held from September 27 to October 15. In contrast to the standard IPC protocol, all participating pyrgeometers were operated by the WRC-IRS staff.

Following a characterisation in the PMOD blackbody BB2007, each pyrgeometer was mounted on the outdoor platform and connected to one of the WRC-IRS dataloggers. A view of the measurement platform is shown in Figure 1 (picture from January 2009). All pyrgeometers were mounted in the Ventilation and Heating units (VHS) developed by PMOD. Apart from two instruments, all were mounted as shaded instruments on solar trackers. The pyrgeometers provided one minute averages of downwelling longwave irradiance during the whole period. Figure 2 shows the quality controlled precipitation-free measurements during the measurement period. The measurements on October 1 and October 5 were flagged by the automatic quality control routine due to rain in these periods and were therefore excluded from the analysis. An extended cloud-free period from October 6 to October 12 also allowed the deployment of the two IRIS radiometers which provided benchmark measurements for an eventual traceability to this potential new longwave irradiance standard. Close to noon on October 6, 7, and 8 several periods of shade-unshade were performed to investigate the influence of direct solar radiation on the performance of unshaded pyrgeometers.

Only three pyrgeometers (labelled noaa, msc, and eppley in the figures) provided an independent calibration performed at the home institution, which are based on a blackbody cavity. The results are shown in Figure 3. The largest differences to the WISG are observed for noaa and msc which underestimate the WISG irradiances by 6 Wm^{-2} during the night and –7 Wm^{-2} during the day, with a variability (95 % percentile), of more than ±2 Wm^{-2} at night and up to ±4.5 Wm^{-2} during the day. On the other hand, eppley has an offset of only +1.6 Wm^{-2} relative to the WISG and a very low variability of ±0.4 Wm^{-2}. Even though this pyrgeometer was operated in an unshaded mode, the day offset is only +0.6 Wm^{-2} with a variability of ±1.9 Wm^{-2}, thus showing an excellent agreement with respect to the WISG pyrgeometers which were operated in a shaded mode.

Figure 1. View of the measurement platform of WRC-IRS on the top of the PMOD observatory. The picture was taking facing South in January 2009. The solar tracker closest to the viewer hosts the World Infrared Standard Group (WISG) of pyrgeometers, while the other two are equipped with customer pyrgeometers.

The remaining pyrgeometers are traceable to the WISG and the comparison of their original calibration is an indication of the long-term stability of these pyrgeometers (and of the WISG). For nighttime data, the offsets to the WISG are between –0.2 Wm^{-2} and +1.4 Wm^{-2} with a 95 % variability between ±0.5 Wm^{-2} and ±1.2 Wm^{-2}. The report of the intercomparison can be found at ftp.pmodwrc.ch → pub → julian → IPgC-I.pdf

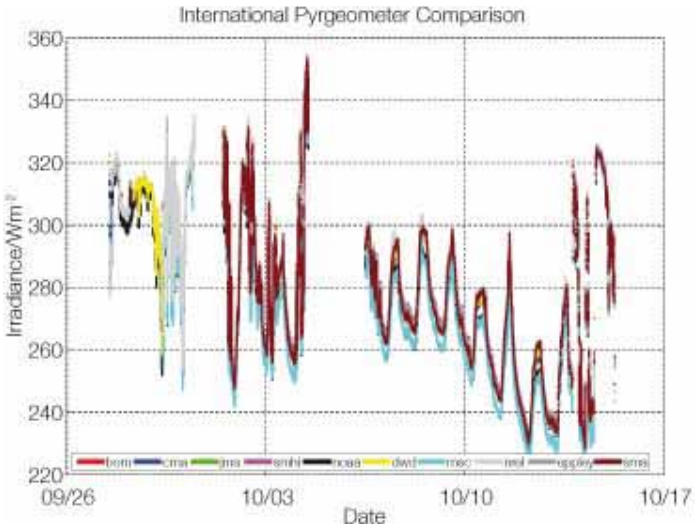

Figure 2. Downwelling longwave irradiance measurements during IPC-XI. The measurements during October 1 and 5 were flagged by the automatic quality control routine and excluded from the dataset due to rain in these periods.

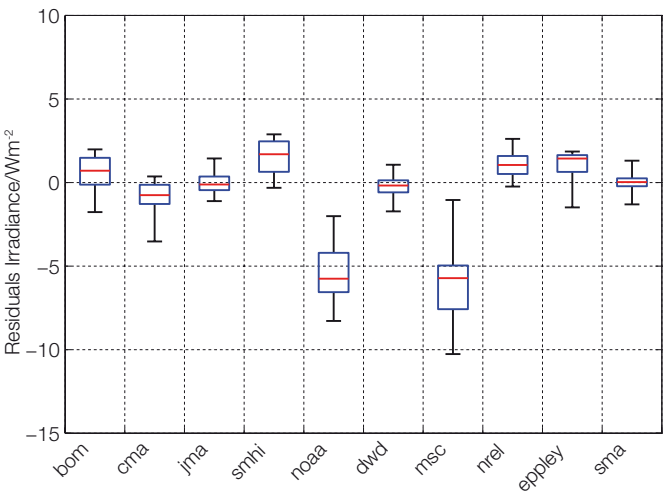

Figure 3. Boxplot of the differences between the pyrgeometer measurements based on the original calibration provided by the participants and the WISG. The pyrgeometers from noaa, msc, and eppley are based on independent calibrations, while all others are traceable to a previous WISG calibration. The whiskers are shown at the 2.5 % and 97.5 % percentiles.

Filter Radiometer Comparisons III

Christoph Wehrli and Stephan Nyeki

The third Filter Radiometer Comparison (FRC-III) Campaign at Davos was successfully conducted in Autumn. Preliminary analyses of FRC-III data show that the excellent agreement found during FRC-II in 2005 was repeated.

In preparation of the 3rd Filter Radiometer Comparison, the PFR instrument N22 at Mauna Loa was exchanged for the newly calibrated PFR N24. This instrument-swap allowed the accuracy of the reference Triad to be verified by Langley calibrations conducted at Mauna Loa. Careful cross-calibration showed that the Triad scale agreed to within ±0.33 % of the Mauna Loa calibration. Thus, one year after incorporation of the Izaña PFR into the Triad, no further adjustment of the WORCC reference scale was deemed necessary.

Figure 1. Some AERONET Skyradiometers participating in Filter Radiometer Comparison III.

FRC-III was held concurrently with the IPC-XI at Davos from 27 September to 15 October, which is conducted on a five-yearly basis. Nine experts from 6 countries participated with 17 instruments (Figure 2). Due to the sunny conditions in the last 2 weeks of the campaign, more than 4'000 simultaneous observations were made on 11 days (> 40'000 measurements). As such, the recommendations made in 2004 at the GAW Davos workshop for instrumental inter-comparisons were accomplished by far. Preliminary analyses of FRC-III data (Figures 3 and 4) show that the excellent agreement found during FRC-II in 2005 was confirmed in 2010.

References: Taylor K. E.: Summarizing multiple aspects of model performance in a single diagram, J. Geophys. Res., 106, D7, 7183–7192, 2001.

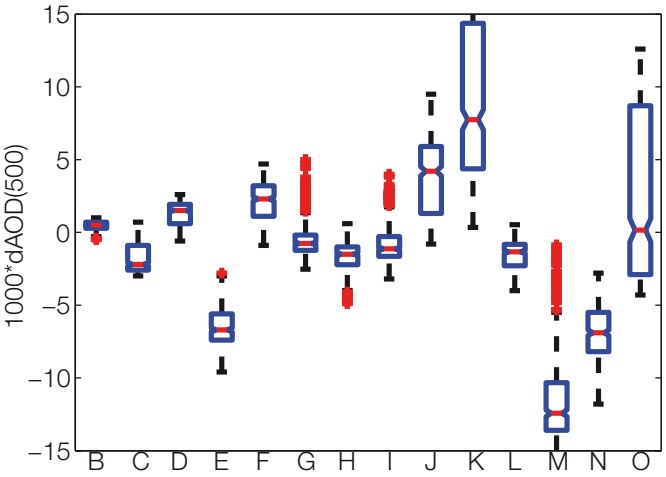

Figure 2. Daily statistics of AOD deviation between participating instruments (B...O) with respect to the WORCC Triad on 8 October 2010. The y-axis represents the uncertainty range recommended by GAW.

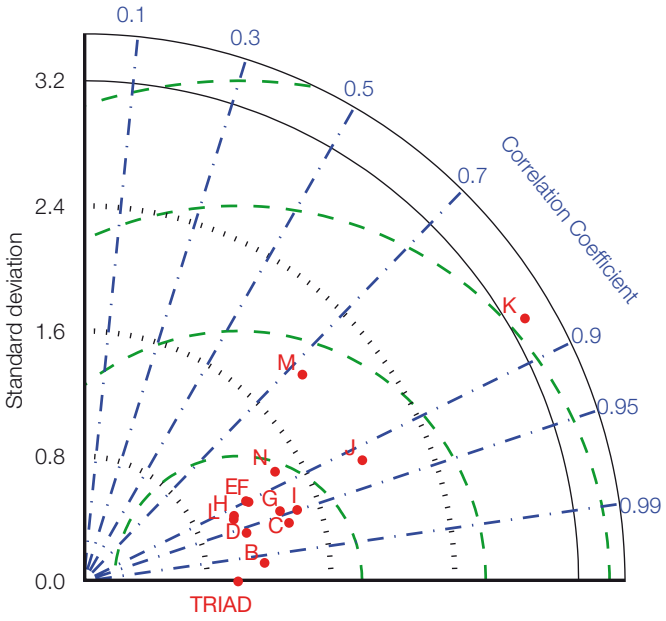

Figure 3. Taylor diagram showing the correlation coefficients (polar angle) and standard deviations (black circles) of participating instruments with respect to the WORCC Triad. Mean differences to the Triad reference can be read from the green circles centered at 'Triad'. All values are given in units of the standard deviation of the instrument 'Triad'.

Operational Services

Quality Management System

Manfred Gyo

PMOD/WRC QMS

Since 2006 the PMOD/WRC maintains an EURAMET approved quality management system based on the general requirements for the competence of testing and calibration laboratories (EN ISO/IEC 17025).

PMOD/WRC is a calibration institute designated by the Swiss National Metrology Institute METAS, and by the World Meteorological Organization WMO, and it is a signatory of the CIPM-MRA (Comité international des poids et mesures – Mutual Recognition Arrangement). To date, the WRC Solar Radiometry Section is covered by the QMS and calibrates customer instruments in accordance with the EN/ISO standard.

Quality Management System Activities

Two calibration and measurement capabilities (CMC) are listed in the database of the „Bureau International des poids et mesures" (BIPM): Responsivity, direct and global solar irradiation.

The UV section of the World Radiation Center prepares for integration of its calibration service in the QMS. In 2010 preparatory work to integrate the EUVC section into the QMS was made and it is intended to get acceptance by EURAMET in 2011.

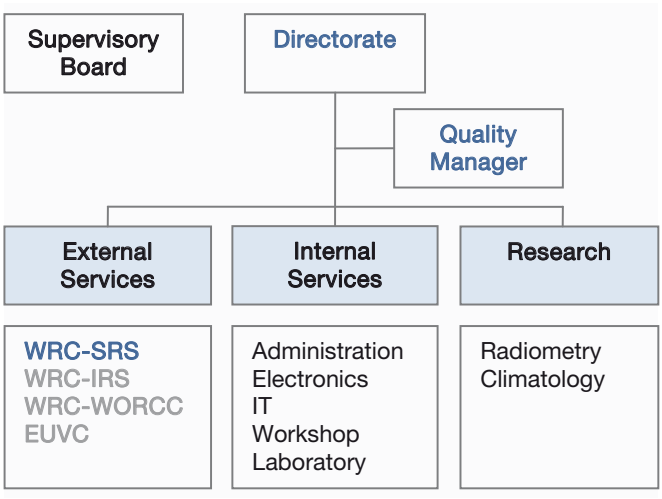

Figure 1. Organizational chart of the PMOD/WRC quality management system. The WRC Solar Radiometry Section performs its calibrations according to the EN ISO/IEC standard 17025.

Calibrations

Manfred Gyo

As in previous years, there was an increase in the number of instrument calibrations in all sections, which reached a total of 216 at the premises of the observatory, and 17 on site calibrations.

Solar Radiometry Section (WRC-SRS)

A further increase of the number of instrument calibrations within this section in 2010 shows good acceptance of this service. A total of 131 calibrations were performed. The WRC section 'Solar Radiometry' calibrated 111 pyranometers, 5 pyrheliometers and 15 actinometers during 76 days of measurement.

Infrared Radiometry Section (WRC-IRS)

The infrared radiometry section of the World Radiation Center calibrated 36 pyrgeometers in 2010. The calibration procedure consists of characterization with a black-body source and direct outdoor comparison of down-welling long-wave irradiance against the World Infrared Standard Group (WISG) of pyrgeometers.

Atmospheric Turbidity Section (WRC-WORCC)

The World Optical depth Research and Calibration Center calibrated 20 Precision Filter Radiometers against the WORCC Triad standard. 6 of these PFR belong to the GAW-PFR network, and 14 to international institutes.

European Ultraviolet Calibration Center (EUVC)

The Ultraviolet Calibration Center of the PMOD/WRC calibrated 10 spectroradiometers at their respective field sites using the traveling reference spectroradiometer QASUME.

Six UVB, 5 UVB/UVA and one UV-Global broadband radiometer were calibrated at PMOD/WRC. During the QASUME site visit in Norway and Finland 17 multi-channel radiometers (NILU and GUV) were calibrated. The QASUME irradiance scale was transferred to three standard lamps at two European institutes.

On July 2010, 7 Brewer spectrophotometers were calibrated relative to the QASUME spectroradiometer during the 5th RBCC-E campaign at Arosa, Switzerland.

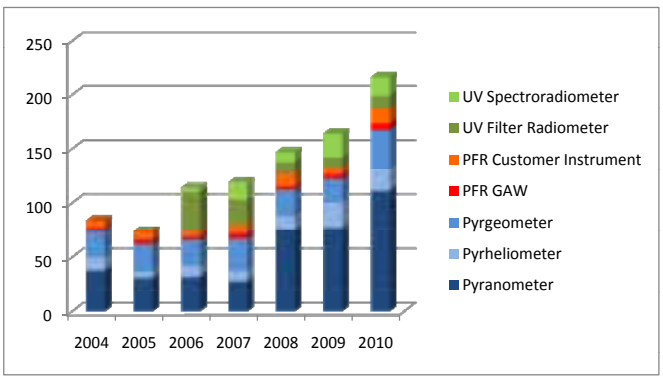

Figure 2. Statistics of instrument calibrations at PMOD/WRC.

Solar Radiometry Section (WRC-SRS)

Wolfgang Finsterle

The Solar Radiometry Section of the WRC (WRC-SRS) is responsible for maintaining and disseminating the World Radiometric Reference (WRR). The WRR is the primary reference for shortwave solar irradiance measurements world-wide. In 2010 the organization of the 11th International Pyrheliometer Comparisons (IPC-XI) was the major task of the WRC-SRS. In view of the increased workload, new control mechanisms were introduced to expedite the commercial calibration services of shortwave radiometers (pyrano- and pyrheliometers). A new data acquisition system was deployed for IPC-XI, offering much more flexibility over the old system including near real-time evaluation of the measurements.

The organization of the 11th International Pyrheliometer Comparison (IPC-XI) started in January with the design of the IPC-XI web site, where participants could register and submit their instrument specifications.

During IPC-XI participants could use a java-based web interface to submit their data. The java interface offered higher flexibility and increased comfort compared to the micro-terminals of previous IPC's. Participants could either connect with their own computer or with a laptop provided by the WRC. A new data acquisition system for the WSG was also deployed for IPC-XI. Besides being more flexible though robust than the old system, it also allows to calculate preliminary results in near real-time. After each series of 21 minutes the ratios of the participating instruments to the WRR were calculated for a quick visual check. Several participating instruments benefited from the prompt identification of instrumental problems. Data loss could be minimized in those instruments. In Figure 1 we show the preliminary new WRR factors for the WSG.

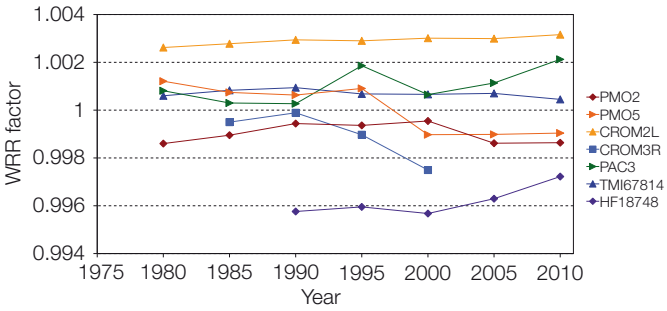

Figure 1. The WRR factors for the WSG instruments since IPC-V (1980). Note that in 2010 the instruments PAC3 and HF18748 were not used to define the new WRR. The WRR factors are preliminary (pending approval by the IPC-XI Ad-hoc Committee).

In view of the increased workload due to the preparations for IPC-XI a simple but effective new control mechanism was introduced to avoid conflicts with commercial calibration services throughout the summer months. Based on the existing database for calibration services a list of calibration deadlines was compiled and checked regularly by the WRC-SRS staff. A flag was risen should the timely return of a customer instrument become questionable. Adequate measures could then be taken to circumvent the conflict. With the ever increasing number of customer instruments this new mechanism will be kept in place also during non-IPC years as an early-warning system and to improve awareness of potential scheduling bottlenecks.

Infrared Radiometry Section (WRC-IRS)

Julian Gröbner

The Infrared Radiometry Section of the WRC maintains and operates the World Infrared Standard Group of Pyrgeometers (WISG) which represents the world-wide reference for atmospheric longwave irradiance measurements.

Performance of the WISG

The WISG operated continuously during the whole of 2010, showing an excellent relative stability between individual instruments of ±1 Wm^{-2}. For the third consecutive year each WISG instrument was calibrated in the PMOD reference blackbody, showing no significant changes in the respective responsivity over this time span. Nevertheless, an internal consistency check of the WISG over the whole deployment period from 2004 to the end of 2010 revealed a slight drift of instrument WISG 4 (CG4 010535) of +1 Wm^{-2} over 7 years, which corresponds to a sensitivity change of approximately –0.14 % per year. WISG4 will be recalibrated in 2011 based on an internal comparison with the WISG reference instruments.

The Infrared Integrating Sphere Radiometer IRIS

The IRIS Radiometers gave consistent measurements within ±2 Wm^{-2} during the whole year. The variability between the WISG and the IRIS radiometers demonstrates a seasonal variability which was already observed in 2009 and which is individual to each WISG pyrgeometer (see Figure 1). The cause of this variability is still under investigation but is probably related to the integrated atmospheric water vapour column as can be seen in Figure 2 where the residuals between each WISG pyrgeometer and the IRIS 2 radiometer are displayed relative to the integrated water vapour.

A Pyrgeometer Intercomparison was held in parallel with the IPC-XI with the participation of 10 pyrgeometers from IPC participants. Please see the corresponding section on page 9 of this report for additional information concerning this event.

Outlook

Three additional IRIS radiometers are in production, two of which have been sold to research groups. The aim is to disseminate this new instrument as a transfer standard between the WRC-IRS and regional calibration centers to serve as reference for pyrgeometer calibrations.

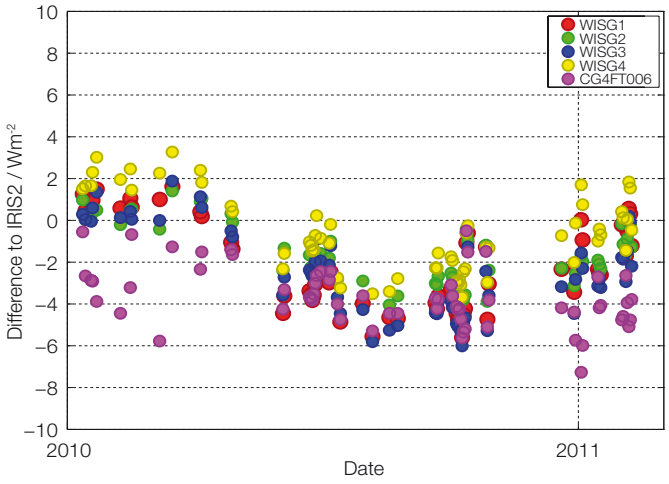

Figure 1. Night average of longwave downward radiation from the WISG pyrgeometers relative to IRIS2 from 1 January 2010 to 9 February 2011.

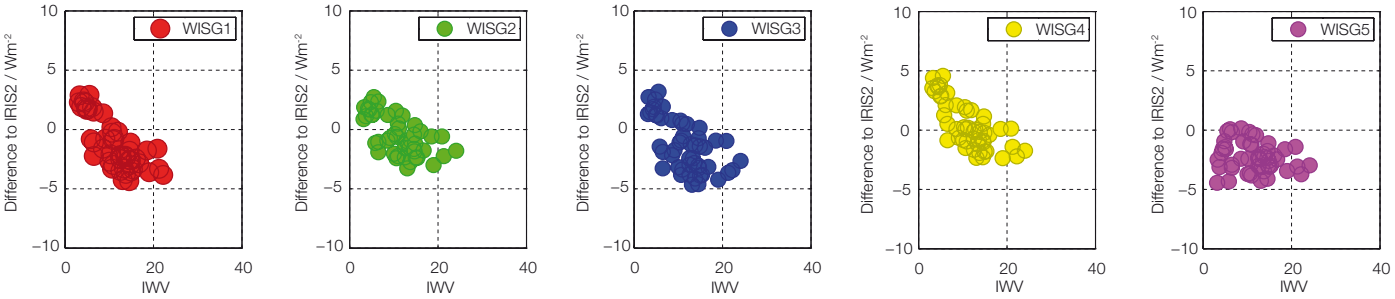

Figure 2. Residuals between each WISG pyrgeometer and the IRIS2 radiometer with respect to the integrated water vapour for the whole of 2011 (51 days).

Atmospheric Turbidity Section (WRC-WORCC)

Christoph Wehrli and Stephan Nyeki

The Atmospheric Turbidity Section of WRC maintains a standard group of 3 Precision Filter Radiometers that serve as reference for Aerosol Optical Depth measurements within WMO. WORCC also operates the global GAW-PFR network of AOD

Three international stations joined the GAW-PFR network in 2010, bringing the total number of stations to 24. Daily AOD results from a number of GAW-PFR stations are now transmitted in (quasi) real time to the WDCA.

With the addition of 3 new PFR sites at Anmyeon (S.Korea, Figure 1), Lindenberg (Germany) and Summit (Greenland) as associate partners, the GAW-PFR network has continued its steady growth and now encompasses 24 stations, twice the number of originally planned stations. A description of all GAW-PFR stations and can be found at www.pmodwrc.ch/worcc. Graphs of annual and time-series aerosol optical depth are available, and are updated each month to allow the early detection of any trends.

The data logger systems from the GAW stations at Danum Valley (Malaysia), Cape Point (South Africa), and Mount Waliguan (China) were recalled to Davos for service and refurbishment. These were returned in a timely manner to prevent the loss of data, but data from Mt. Waliguan (China) were received for only 2 months in 2010.

In 2010, twelve instruments of the extended GAW-PFR network were calibrated against the reference Triad at Davos, and 5 instruments were calibrated by the Langley method at their own measuring sites.

Figure 1. PFR instrument operated by the Korea Global Atmosphere Watch Center at Anmyeon-do Island, South Korea since October 2010.

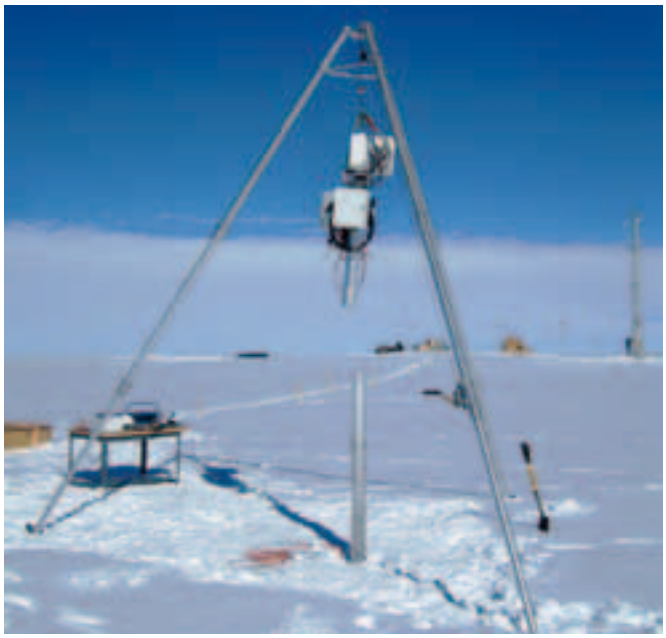

Figure 2. Solar tracker at Summit (Greenland) being reseated to accommodate for snow accumulation.

Only one station audit and AOD inter-comparison campaign was conducted under the EU EUSAAR programme in 2010. Sun-tracker problems resulted in a prolonged campaign at the Birkenes (Norway) super-site, belonging to NILU (Norwegian Institute for Air Research). A campaign was due to be conducted at the Puy de Dome (France) EUSAAR super-site in Autumn but the weather was unsuitable. The campaign was therefore postponed until March 2011.

The CIMEL radiometer at the PMOD, which is part of the AERONET programme, was re-calibrated by PHOTONS, who also processed Level 2 data up to March 2010. The mean bias difference between multi-wavelength AOD at Davos derived from AERONET and the PFR Triad for 2009 was below 0.005, while the root-mean-square scatter was below 0.01 optical depths. These results are very satisfactory, as usual.

Since September 2010, daily AOD results from 16 stations of the GAW-PFR network have been submitted as hourly means and statistics to the WDCA in (quasi) Near Real Time.

These data are available through http://ebas.nilu.no (permission for access should be requested from ebas@nilu.no).

European Ultraviolet Calibration Center (EUVC)

Julian Gröbner and Gregor Hülsen

The Global Atmospheric Watch (GAW) Ultraviolet (UV) calibration center aims at improving the data quality in the European GAW UV network and at harmonising the results from different stations and monitoring programs in order to ensure representative and consistent UV radiation data on a European scale.

In August the broadband UV radiometers located at PMOD/WRC and at the Messfeld-Weissfluhjoch were calibrated relative to the QASUME reference spectroradiometer. The variability of the sensitivities of the five broadband radiometers permanently installed at PMOD/WRC are shown in Figure 1. The most stable radiometers are SL1942, SL1943, and SL3860 from Solar Light with a variability of ±3 % or less since 2007. The radiometer from Yankee Inc., YES010938, on the other hand shows a sudden step change in the fall of 2009 with a sensitivity increase of 8 % and a gradual decrease since then. Finally, the sensitivity of the radiometer from Kipp & Zonen, KZ560, has decreased more or less continuously since 2007, with a sensitivity decrease of 8 % in 3 years. These changes demonstrate the necessity of regular calibrations of UV broadband filter radiometers which can show significant sensitivity changes over a period of only several years.

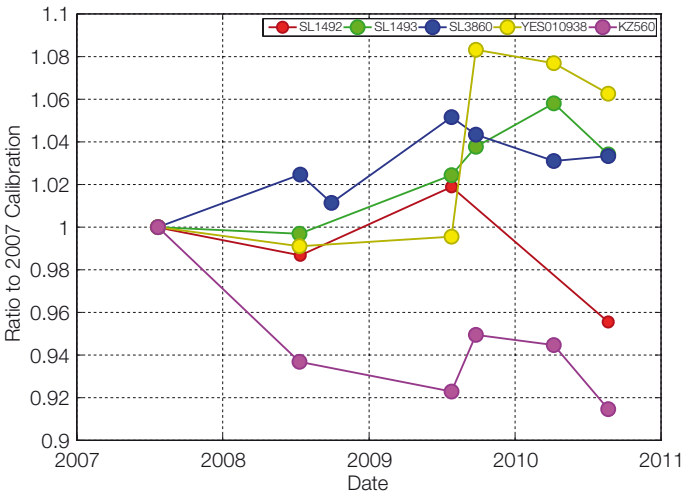

Figure 1. Sensitivity changes of five broadband UV filter radiometers operated permanently at PMOD//WRC. The bullets represent each calibration performed relative to the QASUME reference spectroradiometer.

Quality assurance audits with the transportable reference spectroradiometer QASUME were performed at five sites: The Finnish Meteorological Institute (FMI) in Jokioinen, Finland in May, the University of Oslo, Norway in June, the University of Innsbruck, Austria, in July, the RBCC-E campaign at Arosa, Switzerland in July and the Observatoire de Haute-Provence (OHP), France in September.

Figure 2. Sunrise at Jokioinen during the Nordic Campaign, Finish Meteorological Institute, Finland.

The highlight of 2010 was the Nordic campaign in Finland and Norway in May and June. In addition to the intercomparison of 6 spectroradiometers located throughout Scandinavia, 14 NILU-UV narrowband filter radiometers and three 5-channel GUV radiometers were calibrated relative to the QASUME reference. Among these instruments were the traveling reference instruments used in the African, Tibetan, Chinese, and Nepalese NILU-UV networks managed by the Univ. of Oslo and the Antarctic NILU-UV network managed by FMI.

Results of all the QASUME site audits can be found at the EUVC web-site: www.pmodwrc.ch → WR center → Zusatzbereich EUVC → Qasume Audits

Figure 3. Adjusting the instruments at the University of Oslo, Norway, during the QASUME site audit.

Instrument Development

Instrument Sales

Manfred Gyo

In 2010, four Precision Filter Radiometers (1 Korea, 1 Japan, 1 Canada, 1 WORCC) and five Absolute Radiometers (2 China, 1 Germany, 1 Russia, 1 France) were sold. The production of a new series of PMO6-cc absolute Radiometers began, and the production of a new series of Precision Filter Radiometers was planned.

Figure 1. Mechanic Andreas Schätti.

Photo: Ralph Feiner, Malans.

Spectroradiometer for Spectral Optical Depth

Julian Gröbner

The realisation of a diode-array spectroradiometer for spectral aerosol optical depth measurements in the range 330 to 1045 nm is funded by the Innovationsstiftung of the Kanton of Graubünden. The design study was completed in 2010 and construction and testing of a prototype instrument will be the objective for 2011.

The first year of the project was dedicated to the selection of components and testing of a breadboard version in the optical laboratory of PMOD/WRC. A linear image sensor consisting of 1024 elements from Hamamatsu was chosen as sensing element. The main components which were tested were several concave flat-field corrected holographic gratings used as dispersion element. Following extensive testing, a grating manufactured by Zeiss with 200 lines per mm and corrected for the wavelength range 330 to 1045 nm was selected. In the chosen configuration,

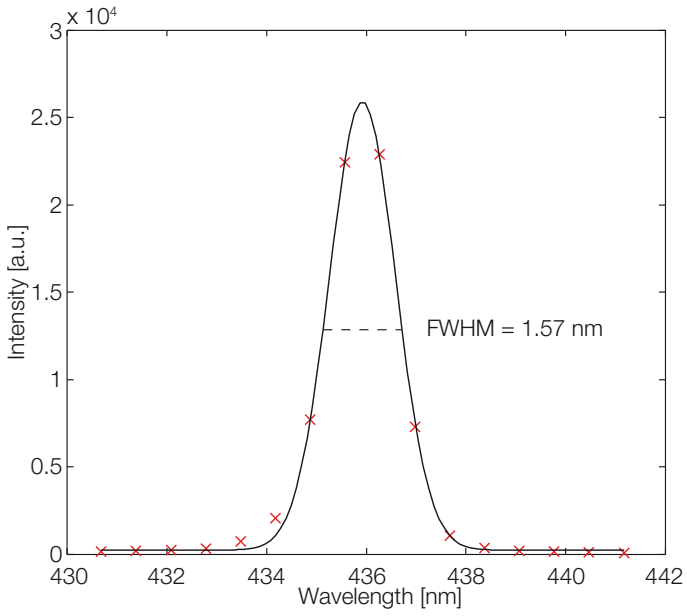

Figure 1. Gaussion fit of the 435.83 nm spectral emission line of a Mercury lamp. The red crosses represent the signals measured by the detectors of the 1024 pixel linear diode-array.

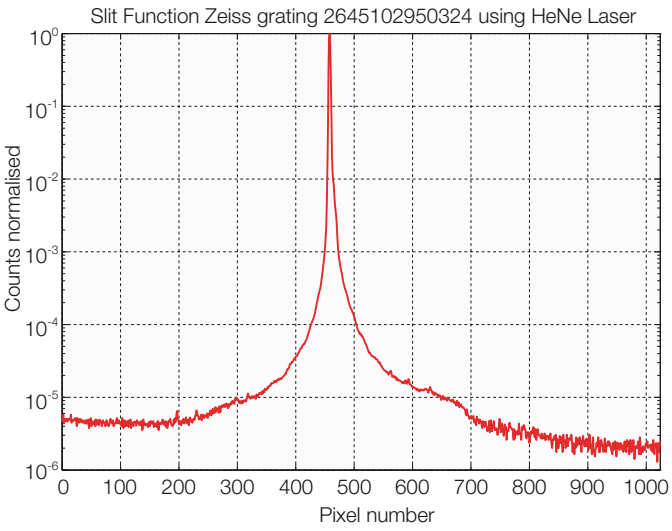

Figure 2. Normalised response to a HeNe laser 633 nm emission line. The remaining far-field stray light measured by the linear diode-array detector is less than 10^{-5}.

using an entrance slit of 50 micrometer, the optical characteristics of the spectroradiometer were determined using a HeNe Laser and emission lines from a mercury discharge lamp. As shown in Figure 1, the resulting spectral resolution at the nominal specifications of the grating as obtained from the manufacturer is 1.57 nm full width at half maximum. The spectral stray light of the open system was determined in the laboratory using the 633 nm emission line of a HeNe Laser. In this setup, a stray light rejection of better than 1 in 100000 could be obtained as is shown in Figure 2 which meets the specifications required for a solar spectroradiometer in the visible to near-infrared wavelength range.

Based on this initial study, a fully operational prototype device will be built in the course of 2011. Outdoor measurements will be expected during the summer months with this instrument and a thorough investigation of its performance under realistic field conditions will provide the required experience for the subsequent realisation of the commercial version of a fully automated spectroradiometer for determination of spectral aerosol optical depth.

Space Experiments

Manfred Gyo, Dany Pfiffner, and Ricco Soder

PREMOS

The experiment PREMOS is a Swiss payload on board the French micro satellite PICARD. The launch of PICARD was on June 15, 2010, and first light on July 27, 2010.

After successful integration of all instruments on the satellite and all system level tests, the satellite was prepared for transportation to Russia for the launch in early 2010.

After the launch preparation at the Dombarovskiy Cosmodrome, located near Yasny, Russia, the launch with a Dnepr-1 rocket took place on June 15, 2010. The Launcher brought PICARD to a polar orbit with an altitude of 725 km and an orbit time of around 100 minutes.

PREMOS was scheduled to be switched on late in the afternoon on June 28, 2010. The switch-on procedures were attended by both Silvio Koller and Dany Pfiffner, during which the covers were also unlocked. Exposure of the instruments was avoided by a slight off pointing from the Sun by the PICARD satellite. All went well and PREMOS stayed in transition mode until June 29, 2010 when it was turned into night mode.

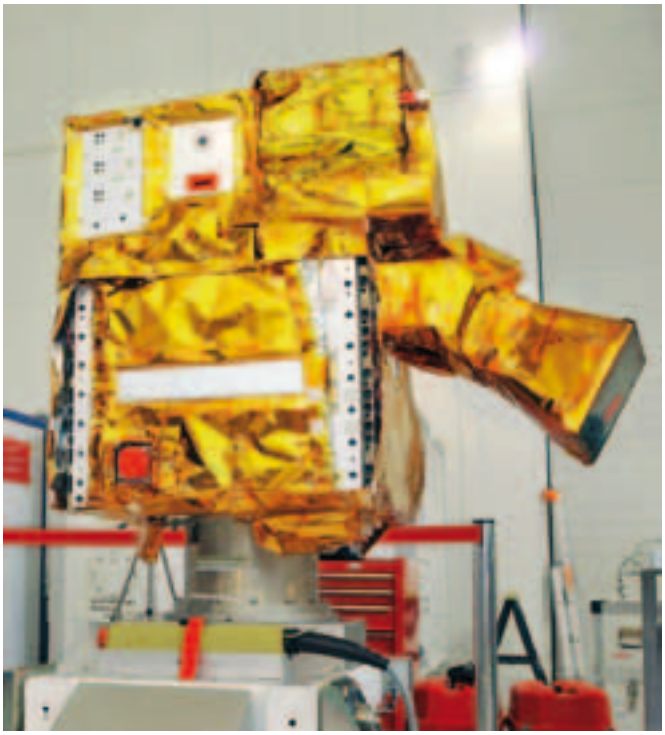

Figure 1. PICARD ready for integration onto the launcher.

After an out-gassing phase of 3 weeks, PREMOS was switched into science mode on July 27, 2010 to take first measurements. First backup measurements were conducted on August 6, 2010, after which PREMOS was set into night mode again for the rest of August. PREMOS has been operating nominally since September 6, 2010, and has delivered continuous measurements with only short interruptions for operational reasons.

An important aspect of data quality control is to assure that on-board temperatures are well-defined and characterized. Figure 2 shows various on-board temperatures over a 150-day period, and illustrates stable and predictable temperature characteristics over the 15 to 40 °C range.

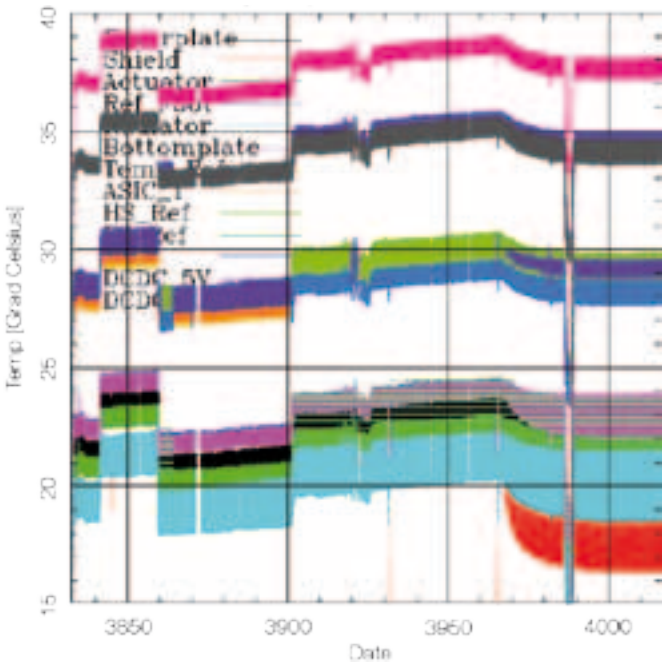

Figure 2. PREMOS on-board temperatures during 2010.

LYRA

The Lyman-Alpha Radiometer is a payload experiment of ESA's technology mission PROBA-2. LYRA contains three UV filter radiometers, each with four channels. Some of them are equipped with BOLD detectors (Blind to the Optical Light Detectors). The PI institute of LYRA is the Royal Observatory of Belgium, ROB. The experiment was built by PMOD/WRC. The project began in 2002 and the flight unit was delivered to Verhaert Space, Belgium in 2007.

On November 2, 2009 the PROBA-2 spacecraft was launched together with the ESA satellite SMOS. Launch and early orbit operations of PROBA-2 were very successful. After a short outgassing phase, LYRA was switched-on in space for the first time on November 16, 2009.

The duration of PROBA-2 nominal operation is 2 years with a further possible extension of 2 years.

First light was observed on January 5, 2010. All three covers were unlocked without a single problem despite the criticality of the operation and were opened one-by-one.

Amongst other observations, first light acquisitions exhibited a strange noise signal in some channels, appearing after each ASIC reload. After several tests, not foreseen during the commissioning phase, the noise problem was solved by closing the cover after every ASIC reload. Subsequently, after many investigations it was decided to disable all ASIC reloads.

After a successful commissioning phase, LYRA has now entered the operational phase with the following repetitive activities:

The nominal operational acquisition is run with Head 2 using an integration time of 50 ms. A calibration is performed each week by measuring the dark and the LED signals.

Each month a backup acquisition is conducted with Heads 1 and 3, as well as a quasi-flat field procedure to determine the sensor homogeneity which can be done by off-pointing the satellite.

Finally, every six months a bake-out phase is planned. All these regular activities allow the solar EUV and FUV irradiances to be monitored continuously with a high temporal resolution.

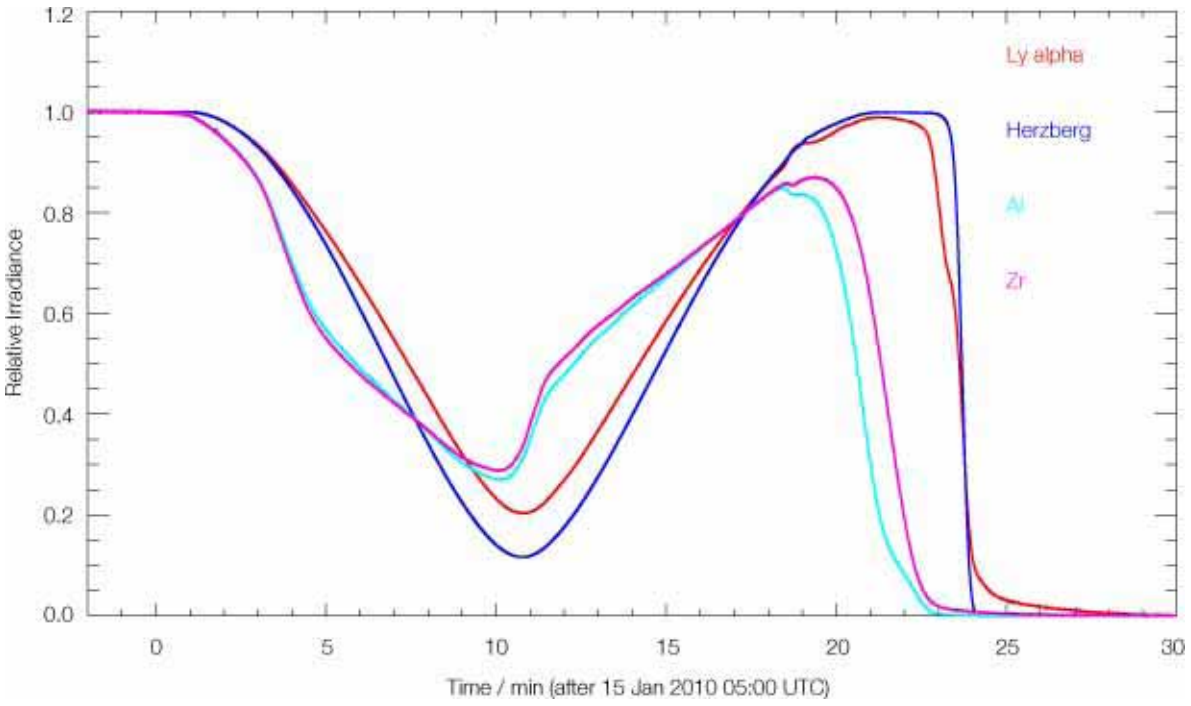

Figure 3. Relative irradiance data of all 4 channels during the solar eclipse on January 15, 2010.

DARA

DARA (Digital Absolute RAdiometer) is a phase B prototype development for an absolute radiometer space experiment on the PROBA-3 satellite. DARA has a completely new design of the cavity and electronics.

Shortly before the start of IPC-XI in October 2010, DARA was ready to be mounted on the big tracker beside the WSG after final assembly of all electronic and mechanical components. Both the on-board software and the ground station software (EGSE) had been tested and were working satisfactorily.

DARA participated in the calibration during IPC-XI in Davos. The instrument proved to be reliable, and high-quality measurements were obtained. Measurements of Solar Irradiance have also been conducted, in addition to operating the instrument in ambient air and under vacuum to determine the non-equivalence.

This new instrument is a very promising design for future ground based and space based measurements of the total solar irradiance.

Figure 4. The new developed cavity implemented within DARA.

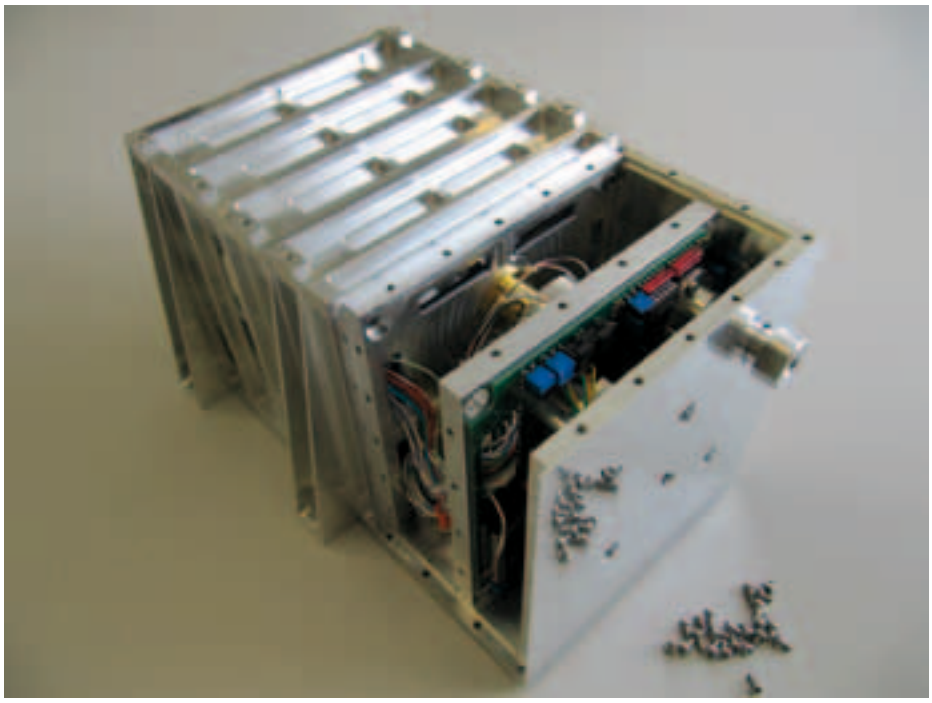

Figure 5. DARA prototype with open view on the electronics.

Scientific Research Activities

Overview

Werner Schmutz

Projects at PMOD/WRC are all related to solar radiation. We address questions in relation to the radiation energy budget in the terrestrial atmosphere as well as problems in solar physics to understand the mechanisms concerning the variability of solar irradiance. Hardware projects at our institute are part of investigations into Sun-Earth interactions by also providing measurements of solar irradiance.

Besides the relevance to the main research themes, there is another important aspect that governs the choice of projects to be conducted at the institute: it is the synergy between operational service tasks and the development of other research activities. Basically, the same instruments are built for space-based experiments as are utilized for ground-based measurements.

The research activities can be grouped into three themes:

- Climate modeling
- Terrestrial radiation balance
- Solar physics

Research activities are financed through third party funding. Last year, we were supported by the Swiss National Science Foundation (3 projects), MeteoSwiss (1 project), the seventh European Framework Program FP7 (1 project), and by the Gebert Rüf foundation (1 project). Hardware development of space experiments is paid by the Swiss PRODEX program (4 projects) and the development of a novel instrument for ground-based applications was supported by the Foundation for Innovation, Development, and Research of the Swiss canton Grisons. These funding sources have supported 6 ongoing PhD Theses, of which one was completed last year, and 3 postdoctoral positions. The institute's PRODEX projects paid for the equivalent of two technical department positions.

A new project started in September 2010. It is a Swiss collaboration project called Future and past solar influence on the terrestrial climate (FUPSOL) with partners from the Institute for Atmosphere and Climate Sciences of the ETH Zürich (IACETH), the Swiss Federal Institute of Aquatic Science and Technology, Dübendorf (EAWAG), the Physics Institute of the University of Bern, and the Oeschger Centre for Climate Change Research of the University of Bern. The project is funded by a Sinergia project of the Swiss National Science foundation and supports five full time positions in total and a 50 % project manager position over the three years of the project. The project manager and one post doctoral researcher are located at the PMOD/WRC.

The launch of ESA's PROBA2 technology mission in 2009, and LYRA first light in January 2010 was already reported in last year's annual report. The commissioning phase of LYRA was successfully completed and the instrument is working nominally. The development of the data pipeline was the task of the PI institute at the Royal Observatory in Belgium. The solar monitoring data of UV irradiance is now finally available to the space weather community in near real time. It is intended that the PMOD/WRC contributes nowcasting of the chemical composition of the terrestrial middle atmosphere in the frame of the SOTERIA FP7 SOTERIA. The required input is the solar irradiance spectrum, which is provided by a French SOTERIA partner from the University of Toulouse. Their pipeline to calculate the solar spectrum from the LYRA data is still not fully completed and thus, the nowcasting at PMOD/WRC is also still in a test phase and not yet publically available. However, we hope that the project will soon be completed as all elements of the final product have been developed. I recommend interested readers to explore and test the visualization software as described by the first science communication in this annual report.

The numerous pages on climate modeling projects testify the high activity and productivity of the climate group at PMOD/WRC. One of their goals is to model and understand the solar influence on climate. For historic times, a required input is the reconstructed temporal behavior of the solar irradiance. As reported in the article by Alexander Shapiro the solar group has come up with a novel approach, which yields a high solar forcing in the past. It will be one of the aims of the FUPSOL project to use this input to explore the consequences on the climate.

On June 15, 2010 the French mission PICARD was launched with four experiments: one of them being a Swiss PI experiment that was built almost completely in-house. The PREMOS instrument package is comprised of absolute radiometers and four channel filter radiometers. PREMOS first light was on July 27, 2010 and the first science highlight is that PREMOS measurements yield a lower solar constant, in significant disagreement with three older space experiments, which are presently still operational, but in agreement with the latest American experiment, TIM on SORCE.

Visualization of the State of the Middle Atmosphere

Tatiana Egorova, Eugene Rozanov, Marco Senft, and Werner Schmutz in collaboration with Nicky Hochmuth, Institut für 4D-Technologien Fachhochschule Nordwestschweiz – Hochschule für Technik

We apply the chemistry-ionosphere climate model (CICM) SOCOL[i] for nowcasting of the state of the middle atmosphere. With this model we are able to simulate the distribution of the temperature and gas species in the upper stratosphere and mesosphere driven by measured or reconstructed spectral solar irradiance. To visualize the nowcasting results and facilitate the analysis we have developed a visualization software.

In collaboration with the Institut für 4D-Technologien Fachhochschule Nordwestschweiz – Hochschule für Technik, we have developed a Viewer which is a browser based visualization software for the nowcasting model CICM SOCOL[i]. The output from the model is a short-term (6-hourly) forecast of the temperature, neutral and charged species and a progressive archive of past calculations. The forecast and archived data are stored in NetCDF format and will be publicly accessible.

The Viewer is the end-user software tool, running in a client web browser, to examine and visualize the space weather data. We have produced a data set to test the Visualization package and created a website for the online Publication of the chemical composition. The Viewer is now integrated into the website: http://projects.pmodwrc.ch/lyra/. With this Viewer it is possible to look at the distribution of some chemical species ("Detail Mode") and their anomalies ("Difference Mode"): menu Nowcast/ Visualization.

Figure 1 illustrates the components of the Viewer:

1. Species selector. Each NetCDF file provides data for the following species: ozone (O3), nitric oxide (NO), nitrogen dioxide (NO2), hydroxyl (OH), water vapor (H2O), electrons (EL), positive ions (PTOT), temperature (TEM), density (DEN), and geopotential height (GPH).

2. Altitude selector: 34 levels can be selected between 500 m and 78.5 km. a) In dependency of the selected species a histogram over the altitude levels is visible. The histogram allows the user to navigate to specific altitude levels with height concentration or intensity.

3. Time settings and animations: a) start day, b) time between each image, c) end date.

4. The data image for the selected species, level and time.

5. Scale: graduation of the color data image with physical units

6. Range mode

7. Detail mode (Figure 2): a) the earth position locator, b) the horizontal chart shows the concentration distribution on the longitude of the selected location, c) the vertical chart shows the concentration distribution for the chosen latitude, d) a chronological time evolution of the selected species at the selected location.

8. Visualization mode: toggle button for 2D or 3D visualization

9. Texture mode: toggle button for a simple or orographical earth texture.

10. Color mode: toggle button for mono or multi color visualization.

11. Difference mode: the image shows the difference between two points in time.

12. Link: the button represents a link to the current application and available settings; therefore it is possible to reopen the application with the same settings.

13. Reload: Initialize reload of the application.

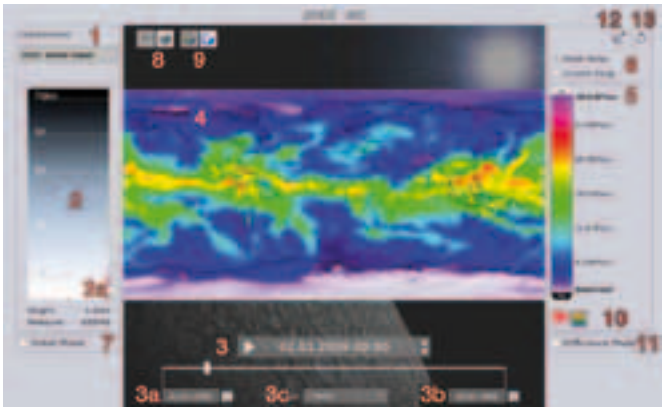

Figure 1. Screenshot of the Viewer with marked components.

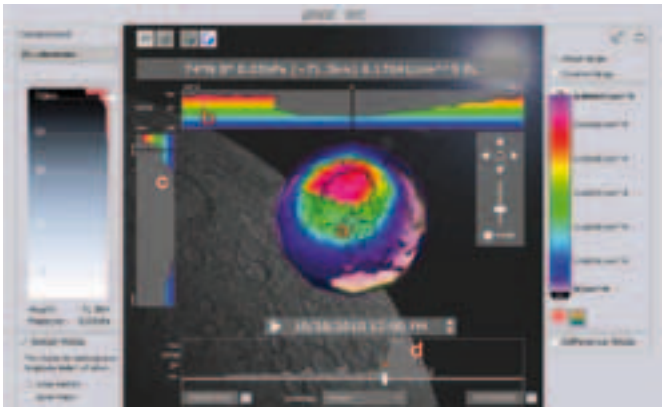

Figure 2. Screenshot of the Viewer in Detail Mode and with 3D visualization.

Development of the Chemistry-Climate Model SOCOL Ver. 3.0

Eugene Rozanov in collaboration with M. Schraner, A. Stenke, and T. Peter, IAC ETH, Zurich

Extensive evaluation of the chemistry-climate model (CCM) SOCOL v2.0 in the framework of the SPARC CCMVal-2 campaign (SPARC, 2010) revealed some deficiencies of the model. We have developed a third version of CCM SOCOL with better treatment of the transport of trace gases. The preliminary evaluation of the new model version shows better performance and closer agreement with available observations.

The SPARC CCMVal-2 campaign (SPARC, 2010) revealed several deficiencies of our CCM SOCOL v 2,0 model. In particular, it was found that the total inorganic chlorine mixing ratio in the southern polar lower stratosphere is still underestimated while in the upper stratosphere it exceeds the maximum amount of total chlorine entering the stratosphere. Schraner et al. (2008) attributed these deficiencies to the problems with the transport treatment and recommended to use a more accurate transport module, which led to the development of the new model version.

The two most important modifications of SOCOL ver.3.0 compared to its predecessors are: (1) The latest version of the middle atmosphere GCM MA-ECHAM5 is used instead of the previous version MA-ECHAM4, and (2) the advection of chemical species is calculated by a state-of-the-art flux-form advection scheme. In contrast to a standard semi-Lagrangian scheme, flux-form schemes are fully mass conservative by design. The scheme is designed for an arbitrary long time step. In addition to mass conservation, this advection scheme satisfies other fundamental requirements for a tracer algorithm such as monotonicity and conservation of tracer correlations, and very effectively prevents numerical diffusion. Another important benefit of the new model version is that the chemistry code was completely rewritten to take advantage of modern, parallel computer architectures.

To evaluate the new CCM SOCOL version we performed a transient simulation from 1975 to 2000, using T31 and T42 horizontal resolutions. The simulation set-up follows the specifications of the CCMVal reference simulation REF-B1 (SPARC, 2010), with the aim of reproducing past atmospheric conditions. The simulation includes several natural and anthropogenic forcings such as the 11-year solar cycle, the quasi-biennial oscillation (QBO), direct radiative and chemical effects of major volcanic eruptions as well as changes in source gas concentrations/fluxes.

The time evolution of the simulated annual mean total chlorine in the surface air and at the stratopause, and the October mean total inorganic chlorine at 50 hPa over the South polar cup is presented in Figure 1 for different model versions and horizontal resolution. The results show that the new treatment of transport allows chlorines in the stratosphere to be better represented: the

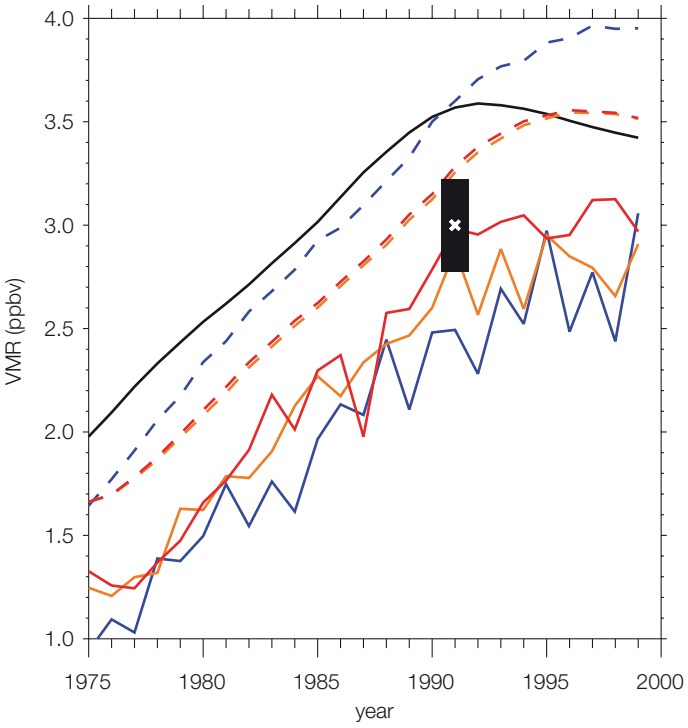

Figure 1. Time evolution of the annual mean total chlorine in the surface air (black solid line) and at the stratopause (dotted lines), and the October mean total inorganic chlorine at 50 hPa over the South polar cup (colored solid lines). The results are from CCM SOCOL ver 2.0 (blue), ver 3.0/T31 (orange) and ver 3.0/T42 (red). The black rectangle represents satellite observations at 50 hPa with 1σ uncertainty.

annual mean total chlorine mixing ratio at the stratopause does exceed the mixing ratio of source gases; total inorganic chlorine in the polar lower stratosphere better matches the observed values.

The new version of the model also shows slightly better representation of the tropical transport and southern polar temperatures in the lower stratosphere, but less accurate heat fluxes over mid-latitudes. More detailed analysis of the model performance is ongoing.

References: Schraner M., Rozanov E., Schnadt Poberaj C., Kenzelmann P., Fischer A., Zubov V., Luo B., Hoyle C., Egorova T., Fueglistaler S., Brönnimann S., Schmutz W., and Peter T., Technical Note: Chemistry-climate model SOCOL: version2.0 with improved transport and chemistry/micro-physics schemes, Atmos. Chem. Phys., 8, 5957-5974, 2008.

SPARC Report on the Evaluation of Chemistry-Climate Models: Eyring V., Shepherd T.G., Waugh D.W. (Eds.), SPARC Report No. 5, WCRP-132, WMO/TD-No. 1526, 2010.

Improvement of the ECHAM5 Solar Radiation Code

Eugene Rozanov, Alexander Shapiro in collaboration with J. Anet (IAC ETH, Zurich), C. Cagnazzo (CEMCC, Bologna, Italy) and M. Giorgetta (MPI, Hamburg, Germany)

We have modified the latest version of the ECHAM5 solar radiation code to better represent the response of the atmospheric heating rates to the variability of the solar spectral irradiance (SSI). The heating rates calculated with both versions are compared against the results of reference calculations using the line-by-line radiation code libRadtran and high resolution SSI, which confirm much better performance of the modified version.

In the framework of our new project FUPSOL we intend to apply our chemistry-climate model SOCOL ver3.0 to study the climate changes caused by the variability of the solar activity. The model is based on the general circulation model ECHAM5. The latest version of the ECHAM5 solar radiation code shows reasonable accuracy of the calculated heating rates but substantially underestimates the response of the solar heating rates to the solar UV variability (SPARC, 2010), therefore its application to studies of solar-climate issues is limited. The problem is most likely related to low resolution of the ECAHM5 radiation code in the UV part of the spectrum (185–250 and 250–440 nm) and can either be solved by a substantial increase in the number of spectral intervals or by application of suitable parameterizations for ozone and oxygen absorption. The computer efficiency of the latter approach is much higher, therefore the latest version of the ECHAM5 solar radiation code contains a set of parameterizations of the heating rates due to solar UV absorption by ozone and oxygen in the atmosphere (Zhu, 1994). The accuracy of the new version of the solar radiation code was evaluated using a reference calculation with the line-by-line libRadtran model (Mayer and Kylling, 2005) driven by high resolution spectral solar irradiance simulated with our COSI model.

The comparison of the reference results with the original and improved version of the ECHAM5 solar radiation code is illustrated in Figure 1. It shows heating rates (HR) and the response of the heating rates to the changes of the solar UV irradiance from the minimum to the maximum of the typical 11-year solar cycle (ΔHR) for the tropical atmosphere case. The solar zenith angle is set to 10° and surface albedo is equal to 10 %. The comparison of the heating rates confirms good performance of the standard ECHAM5 solar radiation code below 60 km. The applied parameterization of the oxygen absorption improves the model accuracy in the mesosphere. The evaluation of ΔHR shows a clear problem with the standard version of the ECHAM5 radiation code mentioned in SPARC (2010). The applied parameterizations of the UV irradiance absorption by oxygen (in the Lyman alpha line, Schumann-Runge bands and Herzberg continuum) and ozone (in the Herzberg continuum, Hartley and Huggins bands) allows the reference results to be represented with much better (but still not perfect) accuracy. It should be noted that the parameterizations described by Zhu (1994) were substantially modified to represent our latest reference calculations performed with the state-of-the-art libRadtran model driven by the solar irradiance with very high spectral resolution and to introduce the dependency of the heating rates on the solar irradiance variability.

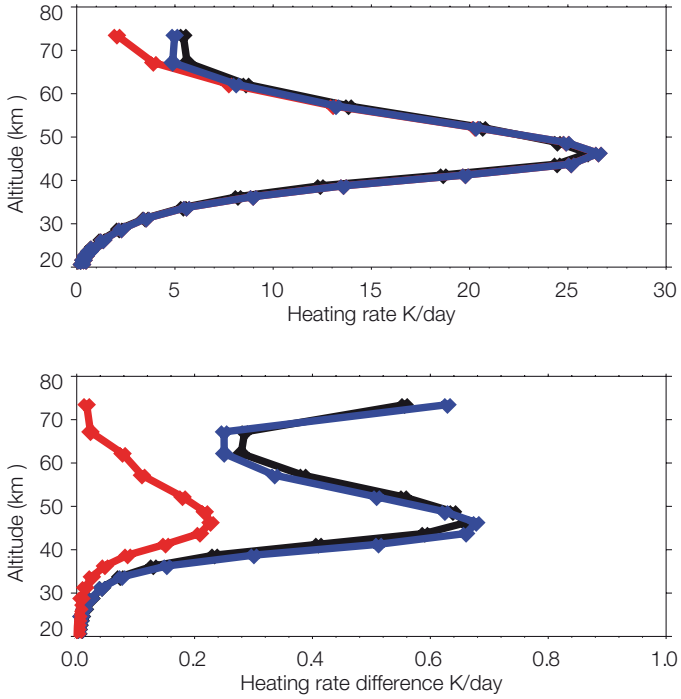

Figure 1. Heating rate (upper panel) and the heating rate difference (lower panel) between solar maximum and solar minimum for the tropical atmosphere and solar zenith angle 10°.The results are from: the reference model (black), the original ECHAM5 version (red) and modified ECHAM5 version (blue).

References:

Mayer B., and Kylling A., 2005. Technical Note: The LibRadtran software package for radiative transfer calculations: Description and examples of use. Atmos. Chem. Phys., 5, 1855–1877.

SPARC Report on the Evaluation of Chemistry-Climate Models: Eyring V., Shepherd T.G., Waugh D.W. (Eds.), SPARC Report No. 5, WCRP-132, WMO/TD-No. 1526, 2010.

Zhu X.: An accurate and efficient radiation algorithm for the middle atmosphere model, JAS, 51, 24, 3593–3614, 1994.

The Chemistry and Climate Response to Energetic Particle Precipitation

Eugene Rozanov in collaboration with M. Calisto and T. Peter, IAC ETH, Zurich

We have applied the chemistry-climate model (CCM) SOCOL v2.0 to evaluate the influence of galactic cosmic rays (GCR), solar protons and low energetic electrons on atmospheric chemistry and the climate. The obtained results reveal significant changes of reactive nitrogen and hydrogen oxides in the mesosphere, middle stratosphere and troposphere mostly over high latitudes followed by localized ozone depletion in the middle atmosphere and ozone production in the troposphere. The results suggest that the energetic particles affect atmospheric chemistry and the climate.

There is some evidence that precipitating particles can substantially perturb the chemical composition of the atmosphere and climate. To quantify these effects we have performed two 46-year (1960–2006) long ensemble transient simulations with the CCM SOCOL v.2.0 (Schraner et al., 2008). The reference run is driven by all commonly applied climate forcings. For the experiment run we extended the set of forcings and included time evolving ionization rates due to GCR, solar proton events (SPE) and low energy electrons (LEE). The comparison of these two runs allows the potential magnitude of the atmospheric parameters response to the introduced energetic particle precipitation (EPP) to be estimated.

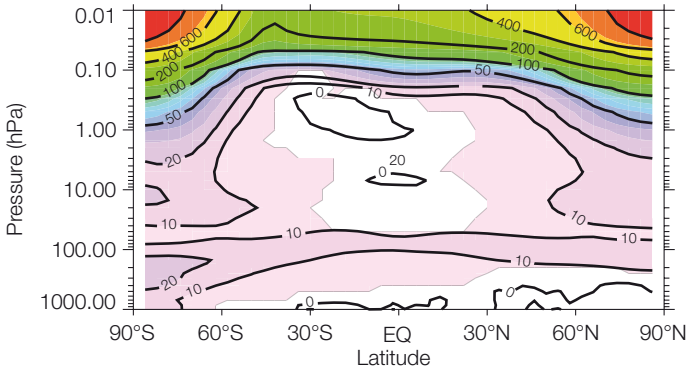

Figure 1. Response of the zonal mean NO_x (%) to the introduced EPP. Coloured areas indicate changes with at least 90% statistical significance.

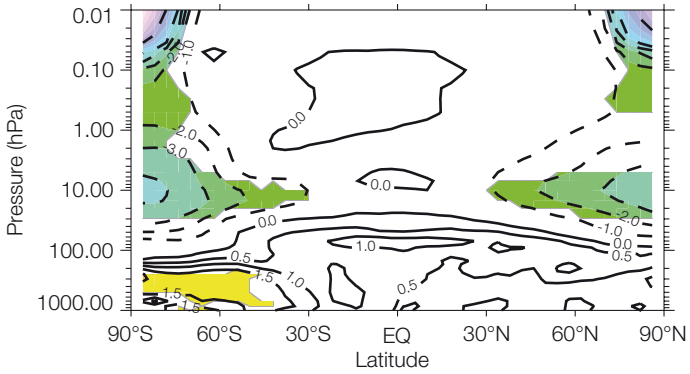

Figure 2. Response of the zonal mean O_3 (%) to the introduced EPP. Coloured areas indicate changes with at least 90% statistical significance.

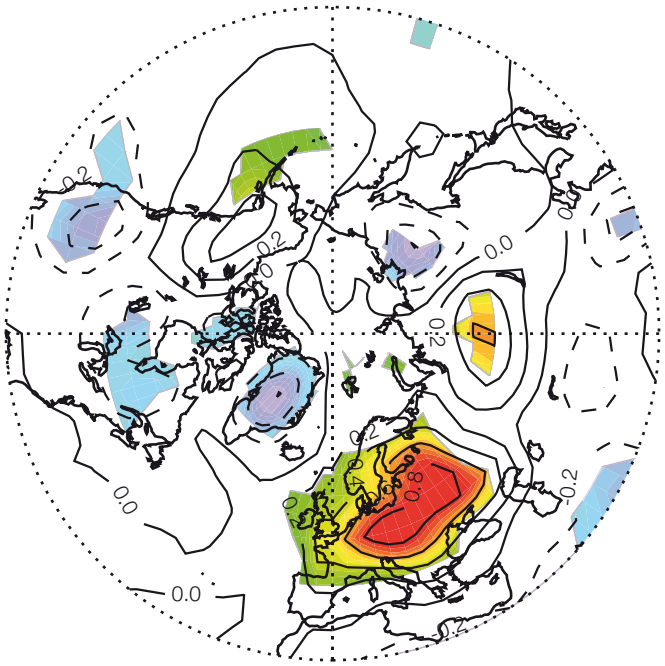

Figure 3. Response of the surface air temperature (K) to the introduced EPP for boreal winter. Coloured areas indicate changes with at least 90% statistical significance.

Figures 1 and 2 illustrate the response of reactive nitrogen (NO_x=NO+NO_2) and ozone calculated as the relative difference between the results of EPP and reference experiments averaged over 46 years of the run. The obtained results reveal significant changes of reactive nitrogen and hydrogen (not shown) oxides in the mesosphere, middle stratosphere and troposphere mostly over high latitude areas followed by localized ozone depletion in the middle atmosphere and ozone production in the troposphere. The perturbation of the atmospheric state induced by the ozone change invokes changes of the surface air temperature leading to pronounced and statistically significant winter time warming up to 1K over Europe, illustrated in Figure 3.

The applied set of EPP does not yet include high-energy magnetospheric electrons which can enhance the effects. A full analysis of the obtained results is in progress.

References: Schraner M., Rozanov E., Schnadt Poberaj C., Kenzelmann P., Fischer A., Zubov V., Luo B., Hoyle C., Egorova T., Fueglistaler S., Brönnimann S., Schmutz W., and Peter T., Technical Note: Chemistry-climate model SOCOL: version2.0 with improved transport and chemistry/micro-physics schemes, Atmos. Chem. Phys., 8, 5957–5974, 2008.

Simulation of a Quiet Period and a Solar Proton Event in October–November 2003

Tatiana Egorova, Eugene Rozanov, and Werner Schmutz

We simulated the changes of the neutral and charged species during October–November 2003 with the chemistry-ionosphere-climate model (CICM) SOCOL[i] to evaluate the model response to changes in solar UV irradiance and particle precipitation. The simulated electron density shows a clear signature of these processes.

In the framework of an international inter-comparison campaign (Funke et al., 2011, accepted) we have simulated the changes of neutral and charged species during October–November 2003 with the chemistry-ionosphere-climate model (CICM) SOCOL[i] driven by: i) the prescribed solar spectral irradiance (SSI), ii) ionization caused by galactic cosmic rays (GCR), and iii) solar proton events (SPE). This period of time is characterized by significant SSI variability due to the solar rotation cycle and contains intensive SPE in October–November 2003. We used the results of this experiment to characterize the response of the electron concentration in the ionospheric layer-D to the short term variability of the solar UV irradiance, and to compare the contribution of different ionization sources to the electron concentration in the middle atmosphere.

Figure 1 shows snap-shots at 12 UTS of the electron density map at ~70 km during a quiet period and SPE. In the absence of SPE the electron density is defined by solar UV irradiance (midday peak values are clearly visible), while intensive SPE substantially (~150 times) increase electron density mostly over the polar caps. The results show that CICM SOCOL[i] driven by solar UV irradiance, GCR and SPE is able to simulate the electron density in the atmosphere.

Ionization of the atmosphere by solar UV irradiance and GCR leads to the build-up of two unambiguous electron layers: one in the mesosphere known as ionospheric layer-D and the other in the middle stratosphere (not shown). Our results also show that sporadic SPE can perturb the electron density even in the tropical middle stratosphere above ~35 km. The electron density in the mesosphere is sensitive to solar activity changes and its imprint can be detected in the simulated results. A solar rotation signature is also visible in the time evolution of short-lived neutral species (e.g., hydroxyl and ozone) in the middle atmosphere.

The comparison of our results with satellite observations showed reasonable model performance in reproducing the formation of nitrogen oxides, and ozone depletion in the lower mesosphere and stratosphere after the SPE. The validation of the electron density response is ongoing.

References: Egorova T., Rozanov E., Ozolin Y., Shapiro A., Calisto M., Peter T., and Schmutz W.: The atmospheric effects of October 2003 solar proton event simulated with the chemistry-climate model SOCOL using complete and parameterized ion chemistry, Journal of Atmospheric and Solar-Terrestrial Physics, 73, 356–365, doi:10.1016/j.jastp.2010.01.009, 2011.

Funke et al., Composition changes after the "Halloween" solar proton event: the High-Energy Particle Precipitation in the Atmosphere (HEPPA) model versus MIPAS data intercomparison study, accepted by Atmos. Chem. Phys., 2011.

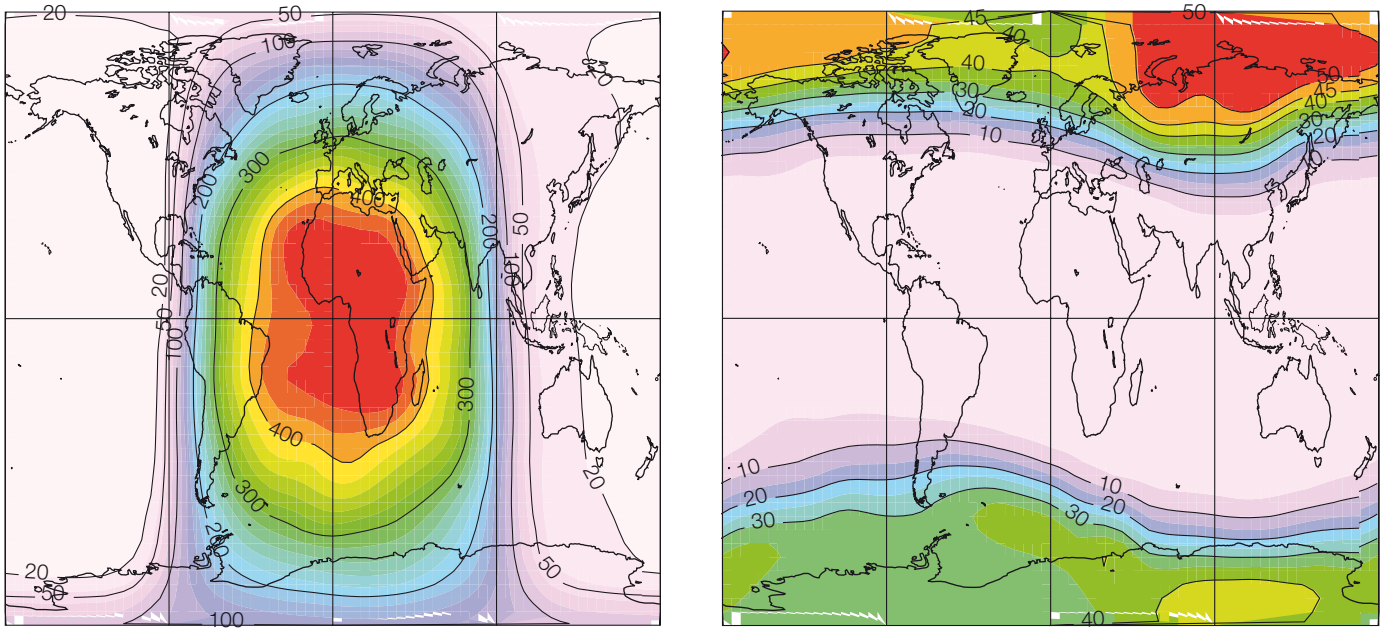

Figure 1. Geographical distribution of the electron density (cm^{-3}) at 12 UTS at ~70 km during a quiet period (before SPE, left panel) and Halloween storm (29.10.2003, right panel, scaled by 10^{-3}).

The Middle Atmospheric Ozone Response to the Uncertainty in the SSI Data

Anna Shapiro, Eugene Rozanov, Alexander Shapiro, and Tatiana Egorova

We simulated the atmospheric response to the Spectral Solar Irradiance (SSI) variability using different SSI datasets with the 3-D chemistry-climate model SOCOL. The experiment covers the period from May 2004 to February 2009. We found that application of the different SSI datasets can lead to a significantly different ozone response.

Recent measurements (obtained by SIM and SOLSTICE instruments onboard the SORCE satellite) show that the variability in UV could be several times higher than all previous estimates. Moreover, the irradiance variability measured by SIM is different from that measured by SOLSTICE in their common spectral region 210–260 nm (Fig. 1). The UV solar flux which penetrates into the middle atmosphere is highly variable and this plays an important role in ozone changes. Thus one can expect that the discrepancy of the SSI data can lead to a difference in the ozone response. We have analyzed the ozone response to three different datasets: the reconstruction by Lean et al. (2005), and two composites of measurements. The first is based on SOLSTICE measurements up to 210 nm and SIM from 210 nm (SIM dominated dataset), and the second one is based on SOLSTICE measurements up to 290 nm and SIM outwards (SOLSTICE dominated dataset).

The analysis of the ozone response to the solar variability is complicated by the presence of the downward trend in the chlorine family concentration (due to the functioning of the Montreal Protocol), which also affects the ozone concentration. To isolate the response to the solar variability we conducted an additional model simulation where the trend due to the solar activity cycle from all datasets was removed. Using this simulation we have excluded all other factors which influence the ozone variability and determined the sensitivity of the ozone changes to the SSI variability (Fig.2).

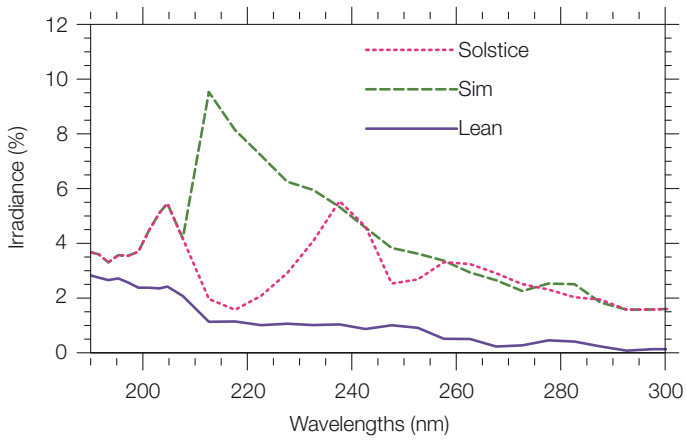

Figure 1. Difference between SSI in 05.2004 and 02.2009 obtained from Lean, SOLSTICE and SIM datasets for 190–300 nm spectral band.

As ozone in the 1–0.05 hPa layer is mostly affected by the irradiance up to 210 nm which is approximately the same for all datasets its variability is similar in simulations with all three datasets. The irradiance from 210–260 nm shows different behavior during the 11-year solar cycle. Due to the oxygen and ozone photolysis which is driven by the solar radiation at these wavelengths the ozone response variability at in the 10–7 hPa layer is also significantly different. Comparison with observations can help to clarify this situation.

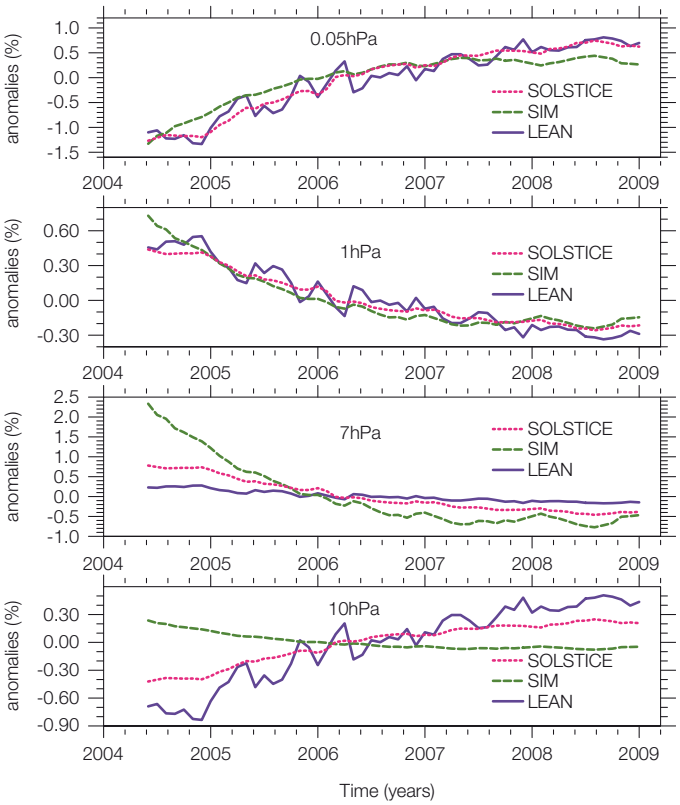

Figure 2. Percentage anomalies of tropical monthly means from 05.2004 to 02.2009 for Lean, SOLSTICE and SIM datasets for different atmospheric layers.

References: Lean J., Rottman G., Harder J., Kopp G.: SORCE contribution to new understanding of global change and solar variability. Solar Physics, 230, 27–53, 2005.

The 27-Day Solar Cycle Signature Observed by MLS (Aura Microwave Limb Sounder)

Anna Shapiro, Eugene Rozanov, and Alexander Shapiro

We analyzed the MLS hydroxyl and water vapor data from August 2004 till December 2005 for the purpose of estimating the zonal mean response of the mesosphere to the 27-day variability of the solar irradiance. We found that the hydroxyl ion shows a positive response to the solar variability, while the response of water vapor is negative.

Hydroxyl is important for the atmospheric chemical balance, and is a fast-reacting and short-lived free radical. Its production in the mesosphere is mostly driven by the photolysis of water vapor. We analyzed the response of MLS hydroxyl and water vapor measurements to solar variability which are available from August 2004 to December 2005. The irradiance was obtained from SOLSTICE/SORCE data.

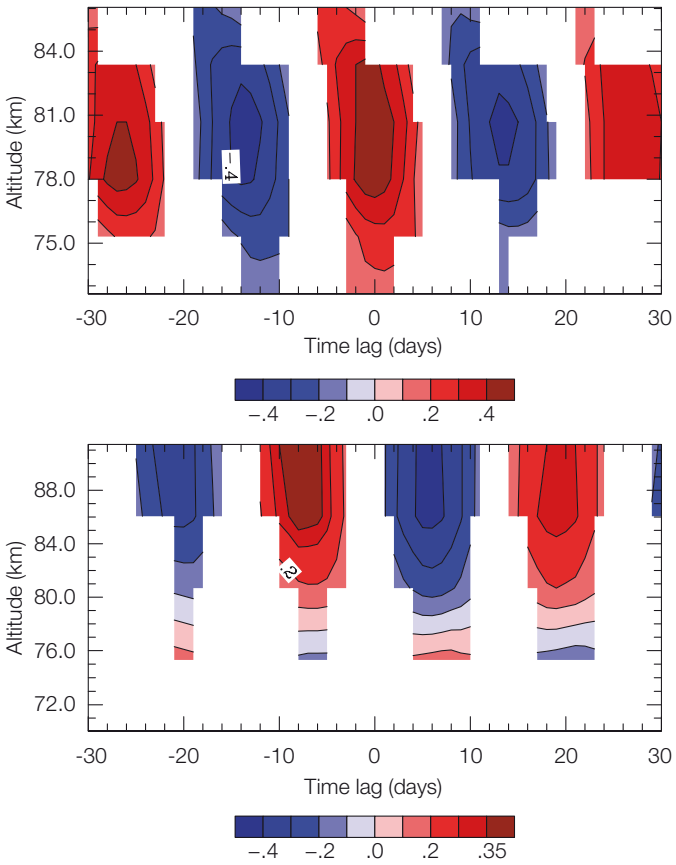

Figure 1. Cross-correlation functions for the daytime tropical mean hydroxyl (upper panel) and water vapor concentrations (lower panel) versus the solar irradiance at the Lyman-α line measured by SOLSTICE/SORCE. The selected areas show the regions where the level of significance is 0.99.

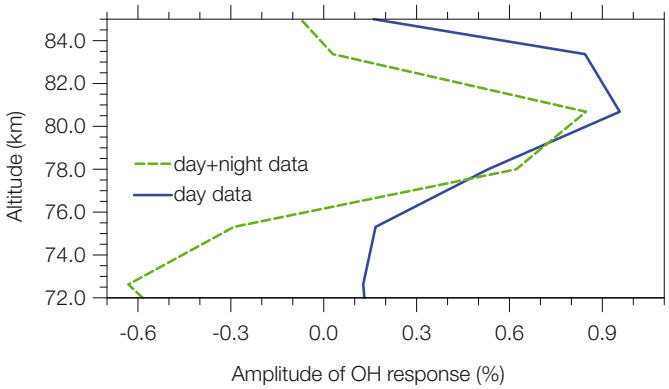

Figure 2. Hydroxyl (upper panel) and water vapor (lower panel) sensitivities (in %) to 1% change of the SOLSTICE/SORCE solar irradiance at the Lyman-α line.

As the lifetime of the hydroxyl ion at 70–85 km is very small in comparison to the 27-day rotational cycle, the response reaches its maximum at about zero time lag (Figure 1, upper panel). The significant correlation (more than 0.5 at 77–83 km) and the positive response at the considered altitudes can be explained by the production of the hydroxyl ion due to photolysis of water vapor ($H_2O+h\nu$ ($\lambda < 200$ nm) $\rightarrow$ H+OH) at these altitudes. The cross-correlation functions for water vapor versus the solar irradiance at the Lyman-α line are presented in the lower panel of Figure 1. They show a strong negative response of water vapor to the solar irradiance 75–90 km altitude range. This can be explained by the destruction of water vapor due to photolysis. The time lag of about 6–7 days corresponds to the lifetime of water vapor at these altitudes.

A sensitivity analysis was conducted both for the hydroxyl and for the water vapor responses (Figure 2). The maximum of the daytime hydroxyl response is reached at ~80 km. However, the response of the data obtained both at night and day is smaller and almost zero at altitudes higher than 81 km. The sensitivity of water vapor to the Lyman-α irradiance change is negative and reaches –0.9 at about 90 km. The day-time+night-time and day-time water vapor sensitivities are almost identical at altitudes higher than 80 km due to its long lifetime.

Attribution of Stratospheric Changes during 21st Century

Eugene Rozanov, Tatiana Egorova in collaboration with V. Zubov and I. Karol, MGO, St. Petersburg, Russia

We have performed a series of sensitivity experiments with the chemistry-climate model (CCM) SOCOL in time-slice mode to attribute previously obtained changes in the stratosphere during 21st century. We have found that the warming of the ocean surface is largely responsible for the acceleration of meridional circulation and temperature changes in the troposphere, tropical lower stratosphere and polar stratosphere below ~40 km.

The majority of CCMs participating in the CCMVal-2 intercomparison campaign predicted an intensification of the Brewer-Dobson circulation (BDC) in the future which resulted in a pronounced increase of the total ozone over the extratropical areas, ozone decrease and cooling in the tropical lower stratosphere (SPARC, 2010). Physical mechanisms responsible for this phenomenon have not been yet clearly identified and there is still no consensus whether it is the result of greenhouse gas induced tropospheric warming or stratospheric cooling. To elucidate the causes of this effect we performed a series of time-slice sensitivity runs with CCM SOCOL (Schraner et al., 2008) for the years 2000, 2050 and 2100. The reference run with all anthropogenic forcings confirmed the results of the transient simulations. For the attribution of the future changes we consecutively kept constant one of the applied forcings: greenhouse gases (GHG); ozone destroying substances (ODS); sea surface temperature and sea ice concentration (SST/SI).

Figure 1 illustrates the vertical profiles of the zonal mean temperature difference between boreal winters of 2100 and 2050 obtained from the results of reference run and experiments with fixed GHG (noGHG) and SST/SI (noSST) forcings. The choice of the time interval was made to cover the period with minor ODS changes to emphasize the role of GHG and SST.

The results showed that the cooling of the extrapolar stratosphere is mostly related to the increase of GHG in this region, while the changes of the SST/SI play a major role in the troposphere, tropical lower stratosphere and polar stratosphere below ~40 km. Dipole-like temperature changes reflect deceleration of the polar night jet and intensification of the BDC. They do not appear in the noSST experiment suggesting that, at least in our model, the intensification of the BDC in the future is caused by enhanced wave generation in the troposphere.

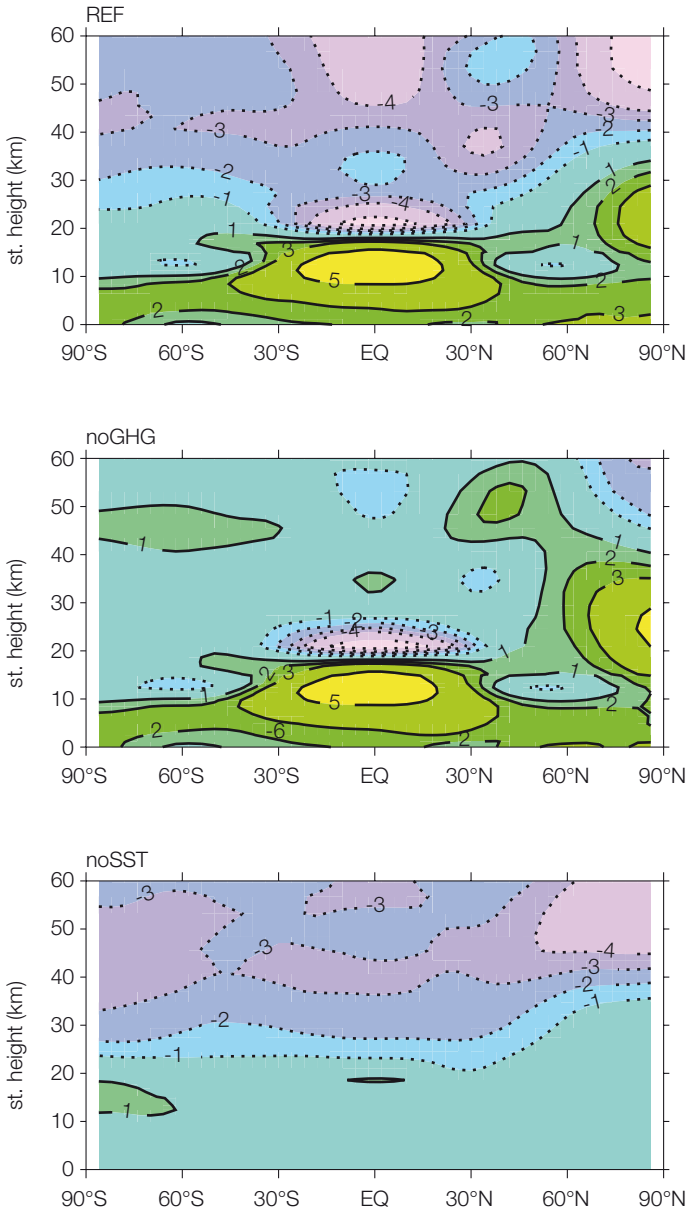

Figure 1. Zonal mean temperature difference (K) between boreal winters in 2100 and 2050 obtained from the results of reference run and experiments with fixed GHG (noGHG) and SST/SI (noSST) forcings.

References: Schraner M., Rozanov E., Schnadt Poberaj C., Kenzelmann P., Fischer A., Zubov V., Luo B., Hoyle C., Egorova T., Fueglistaler S., Brönnimann S., Schmutz W., and Peter T.: Technical Note: Chemistry-climate model SOCOL: version2.0 with improved transport and chemistry/micro-physics schemes, Atmos. Chem. Phys., 8, 5957–5974, 2008.

SPARC Report on the Evaluation of Chemistry-Climate Models, Eyring V., Shepherd T.G., Waugh D.W. (Eds.): SPARC Report No. 5, WCRP-132, WMO/TD-No. 1526, 2010.

Present-Day Benefits of the Montreal Protocol Limitations

Tatiana Egorova, Eugene Rozanov, and Werner Schmutz in collaboration with IAC ETH, Zurich and MGO, S. Petersburg, Russia

We present an analysis of the simulations performed using the chemistry-climate model (CCM) SOCOL with and without Montreal Protocol and it's Amendments (MPA) restrictions. Here we show present-day benefits of MPA regulations for total ozone.

We conducted two model simulations with CCM SOCOL (Schraner et al., 2008): the first simulation used actual values of ODS emissions (scenario A1 from (WMO, 2007)) and the second used ODS concentrations prescribed according to the scenario by Velders et al. (2007), suggesting an ODS increase by ~3 % per year due to the absence of MPA.

Figure 1 illustrates the time evolution of monthly mean total ozone saved by MPA from 2000 to 2011. We find that the MPA has saved 10–30 % of the present-day total ozone in the Northern and Southern Hemispheres. In the tropical and extra tropical latitudes the amount of saved ozone exceeds 5 %.

The geographical distribution of the annual-mean total ozone destruction prevented by the MPA is presented in Figure 2. Model results for 2009 show maximum benefits for the Northern Hemisphere due to MPA implementation which is more than 25 %. For Northern Europe the benefits are about 8–15 %. In the Southern Hemisphere the largest benefits during the last 10 years were obtained in 2003, which reaches more than 30 %.

Figures 1 and 2 also show that for the present-day total ozone the effect of MPA limitations on man-made chlorofluorocarbons depends not only on the amount of chlorine loading but also on the meteorological conditions and is more pronounced for a colder stratospheric winter.

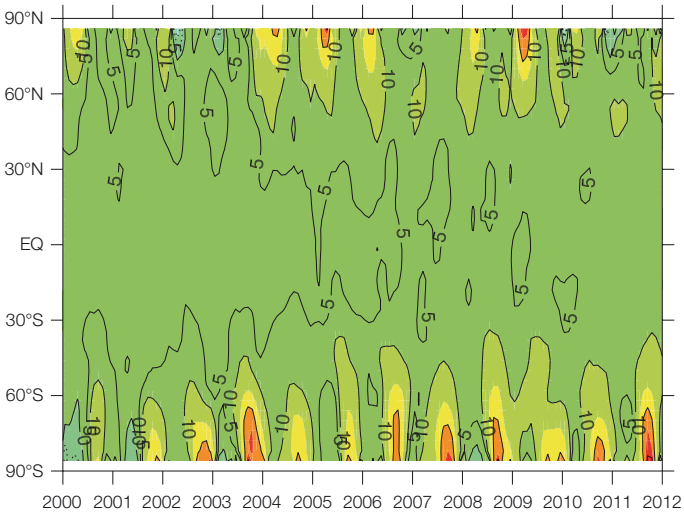

Figure 1. Simulated monthly mean evolution of the total ozone distribution prevented by the MPA. The values for isolines in percent are: 5, 10, 30.

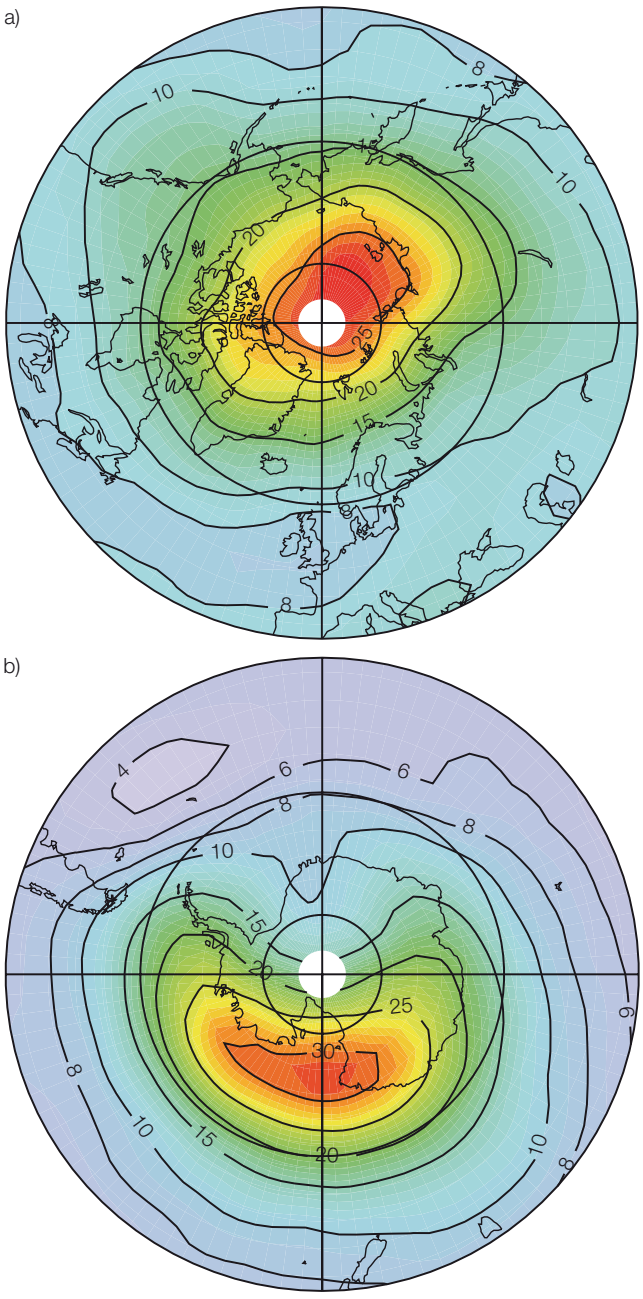

Figure 2. Geographical distribution of the annual-mean total ozone destruction prevented by the MPA for the Northern Hemisphere in 2009 (a), and for Southern Hemisphere in 2003 (b). The values for isolines in percent are: 4, 6, 8, 10, 15, 20, 25.

References:

Schraner M., et al.: Technical Note: Chemistry-climate model SOCOL: version2.0 with improved transport and chemistry/micro-physics schemes, Atmos. Chem. Phys., 8, 5957–5974, 2008.

Velders G.J.M., Andersen S.O., Daniel J.S., Fahey D.W., and McFarland M.: The importance of the Montreal Protocol in protecting climate, Proc. Natl. Acad. Sci. USA, 104(12), 4814–4819, 10.1073/pnas.0610328104, 2007.

World Meteorological Organization (WMO) (2007), Scientific 971 Assessment of Ozone Depletion: 2006, Report No. 50, 572pp, Geneva, Switzerland.

Erythemally weighted Irradiances for Montreal and No Montreal Protocol Conditions: 1960 to 2100

Julian Gröbner, Matthias Hauser, Eugene Rozanov, and Tatania Egorova

We describe the influence of the Montreal Protocol on erythemally weighted UV irradiances in the period 1960 to 2100 using the chemistry climate Model (CCM) SOCOL.

In order to assess the influence of the Montreal Protocol on UV radiation, two different runs of CCM SOCOL were evaluated. The first has the emission of ozone depleting substances (ODS) set according to the restrictions of the Montreal Protocol and all its amendments (MPA) while the second run allowed the ODS to grow by 3 % annually (noMPA). To measure the change in incoming UV radiation, erythemally weighted irradiances (Eery) were calculated for the whole globe.

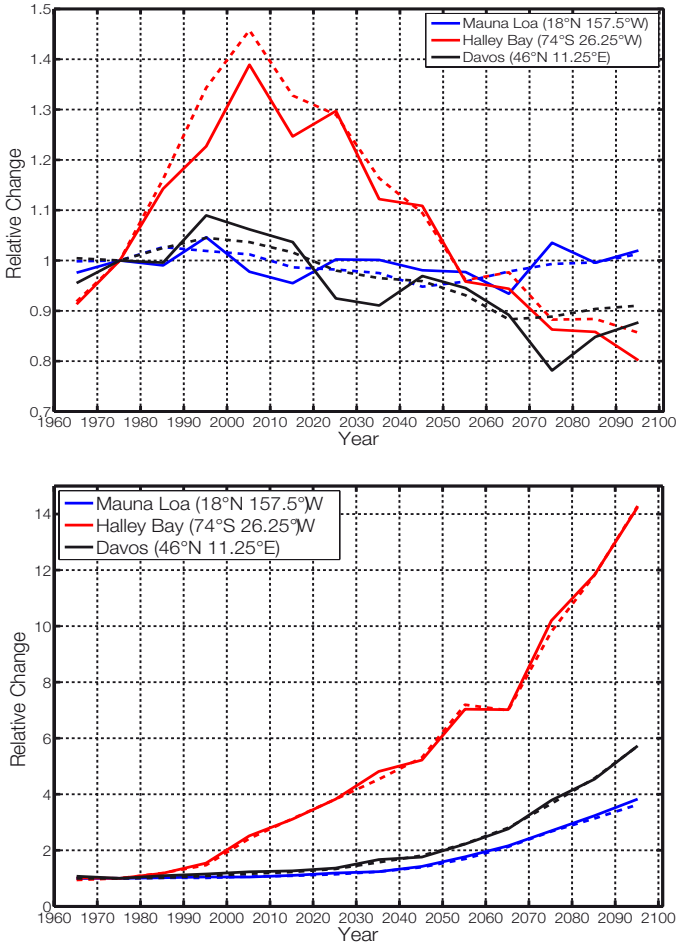

Figure 1. Decadal mean of Eery for Mauna Loa (March), Davos (March) and Halley Bay (September) 1960–2100 relative to the mean of 1970–1979. (a) shows the MPA, (b) the noMPA. Solid line is with cloud modification factor, dashed line without.

Both scenarios have the long-lived greenhouse gas surface concentrations set according to the A1B scenario of SRES (Special Report on Emission Scenarios, IPCC, 2001 [1]). The difference between the two runs is that the noMPA has a modelled annual increase of ODS of 3 %. As we are only interested in the influences of human activity, all external forcings (volcanic eruptions, solar

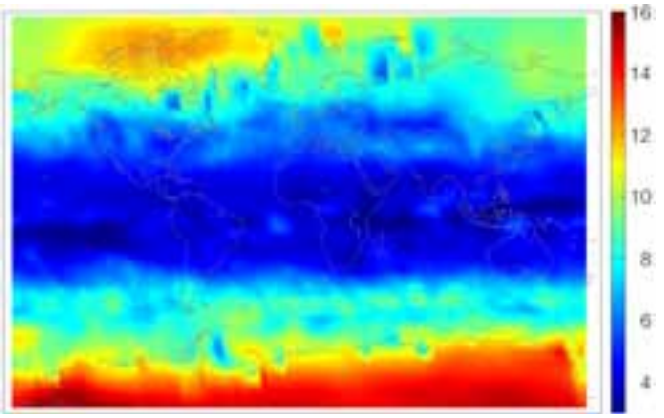

Figure 2. Erythemally weighted irradiance in March 2099 relative to 1970 for the noMPA case.

variability etc.) are turned off. The SOCOL data is available as monthly means on a grid of 4 x 3.75 degrees (latitude x longitude) and extends up to 0.1 hPa in 39 levels. SOCOL outputs total column ozone, ozone and temperature profile, albedo and surface pressure which were used as inputs to the Radiation Transfer Model libRadtran [2] to calculate the erythemally weighted irradiances at every gridpoint.

The UV spectra were calculated for local noon when the UV radiation is highest, and for clear sky situations. The conversion to cloudy sky was obtained by applying a cloud modification factor to the clear-sky calculations. The cloud modification factors were determined from the shortwave radiation outputs of SOCOL and converted to UV cloud modification factors using the relationship determined in [3].

For the scenario including the Montreal Protocol it is found that Eery decreases (by a maximum factor of 0.65) at latitudes higher than 30° for cloud free-skies up to 2099, whilst at latitudes lower than 30° it increases slightly (maximum factor of 1.1) compared to 2010. Including the influence of clouds yields a similar result at high latitudes but obscures the trend observed in the tropics (see Figure 1a). For the noMPA simulation, Eery increases steadily, the Central European value in 2100 is almost 6 times larger than the value modelled for 2010 (Figure 1b). This increase is more pronounced at high latitudes (Antarctic Eery would increase more than 14 times in the same period (Figure 2).

References:

[1] Nakicenovic N., et al.: 2000, Emissions Scenarios. IPCC, Cambridge University Press, 570 pp.

[2] Mayer B., Kylling A.: 2005, Technical note: The libRadtran software package for radiative transfer calculations – description and examples of use, Atmos. Chem. Phys., 5, 1855–1877, doi:10.5194/acp-5-1855-2005.

[3] den Outer P.N., Slaper H., Tax R.B.: 2005, UV radiation in the Netherlands: Assessing long-term variability and trends in relation to ozone and clouds. Journal of Geophysical Research-atmospheres, 110, D02 203.

Stability and Accuracy of UV Broadband Radiometers

Gregor Hülsen and Julian Gröbner

We describe the stability and accuracy of Broadband UV Radiometers. Drifts of the sensitivity exceeding 2 % per year are observed. The expanded instrumental uncertainty is on the order of 9 % and can be achieved with annual calibrations.

The European UV Calibration Center (EUVC) at PMOD/WRC maintains a triad of reference broadband radiometers: Solar Light 501 (SL 1493), Kipp & Zonen UV-S-E-T (KZ 560) and Yankee UVB-1 (YES 010938). The radiometers have been installed since January 2007 on the PMOD/WRC roof and record Erythemal weighted UV irradiance. The instrument raw data is first processed using the calibration factors obtained in summer 2006 (level3-2006). A second dataset is calculated using all calibrations since then – with a linear interpolation between the calibration periods (level3).

The instruments are calibrated at least annually. The spectral and angular responses are determined in the laboratory and the absolute calibration is obtained outdoors by measurements relative to the reference spectroradiometer QASUME [1]. The uncertainty of the radiometers during the calibration periods is around 6 % (see table 1).

The level3 and level3-2006 datasets are compared with the UV irradiance data recorded by spectrophotometer Brewer #163 since 2007. The Brewer is calibrated relative to the EUVC irradiance scale using 1000W DXW lamps once per year. Outdoor re-calibrations are performed monthly using 250W travel standard lamps.

Figure 1 shows the ratio of the radiometer measurements relative to the reference spectrophotometer measurements as daily means, where only the first calibration in the year 2006 was used. The 95 % variability is listed in Table 1. The sensitivity of the KZ has increased by about 10 % whereas the other two instruments decreased in sensitivity by about 5 %.

Figure 2 shows the performance of the radiometers using all calibrations in the selected period. As shown in Table 1, the instruments show a short-term expanded uncertainty (90 days) after the calibration of 6.1 % to 6.5 %. Using annual recalibrations the expanded uncertainty is on the order of 9 %.

	U(Level3-2006) [%]	*U(Level3) [%]*	*U(Certificate) [%]*	*U(90) [%]*	*U(annuall) [%]*
SL	*6.9*	*6.1*	*5.7*	*6.6*	*8.3*
KZ	*9.6*	*6.5*	*5.9*	*7.0*	*8.8*
YES	*8.2*	*6.4*	*6.7*	*7.4*	*9.2*

Table 1. Variability of Broadband radiometer measurements for the two datasets, the uncertainty of the calibration, the expanded uncertainty for the first 90 days after calibration and the annual uncertainty.

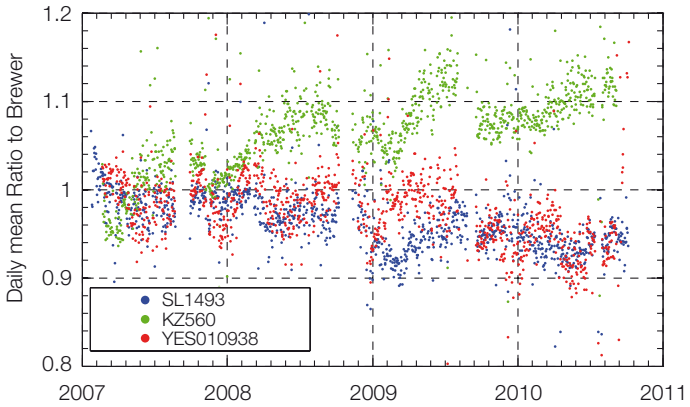

Figure 1. Broadband radiometer data relative to the Brewer spectrophotometer measurements (level3-2006 dataset).

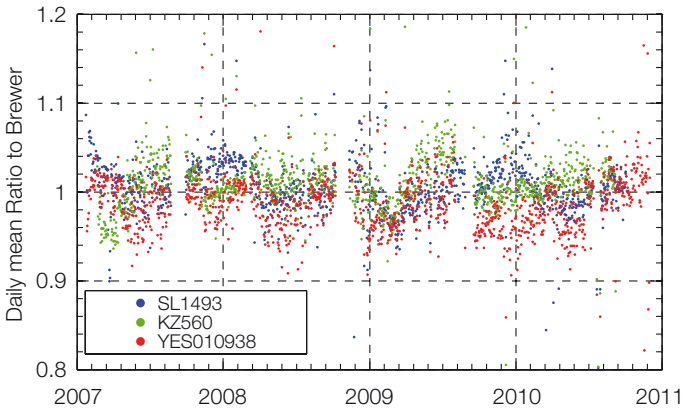

Figure 2. Broadband radiometer data relative to the Brewer spectrophotometer measurements (level3 dataset).

References: Hülsen G., Gröbner J.: 2007, Characterization and calibration of ultraviolet broadband radiometers measuring erythemally weighted irradiance, Appl. Optics 46, 5877–5886.

Parametrization of Cloud-Free Down-Welling Long-Wave Radiation

Stefan Wacker and Julian Gröbner

We improved the performance of commonly used empirical schemes to calculate down-welling long-wave radiation (DLR) by incorporating the measured temperature lapse rate into these models. Furthermore, we developed a new DLR model which calculates the DLR without any empirical factors.

The parameterization of DLR has been widely studied over the years. Parameterizations are essential to validate satellite-derived long-wave surface fluxes and long-wave outputs from climate models. Furthermore, in order to determine the effect of clouds on the long-wave irradiance, one needs accurate models in order to quantify the hypothetical cloud-free fluxes during cloudy periods.

Most of these long-wave models use screen level temperature and humidity to calculate DLR because about 90 % of DLR stems from the first km above ground referred to as the atmospheric boundary layer (ABL). Thus, these formulae do not consider the diurnal variability of the temperature lapse rate and hence DLR in the ABL. Therefore, most of these schemes have considerable large uncertainties.

Gröbner et al. (2009) showed that the lapse rate in the ABL can be derived from pyrgeometer measurements. We included monthly means of the lapse rate into two widely used models, the formulae of Brutsaert (1975) and Prata (1996). Moreover, the scheme of Dupont (2008) was used which uses an empirical derivation of the lapse rate. Finally, we developed a new long-wave model which is based on radiative transfer theory in the 8–14 µm wavelength range (main atmospheric window). Outside the atmospheric window, the DLR is calculated assuming Planck's law and corrected for the instantaneous integrated water vapor content (IWV) using the function f (IWV):

$$DLR = \int_{3\,\mu m}^{8\,\mu m} L(T_{ABL},\lambda)d\lambda + DLR_{8-14\,\mu m} + \int_{14\,\mu m}^{\infty} L(T_{ABL},\lambda)d\lambda - f(IWV),$$

where L is the Planck function and T_{ABL} the effective radiating temperature of the atmosphere. T_{ABL} can be derived from pyrgeometer measurements (see Gröbner, 2009).

We compared the calculated DLR fluxes to observations at four stations. Results revealed that the standard deviation of the empirical models can be reduced by up to 40 %, when the diurnal variability of the lapse rate is included in the Brutsaert and Prata models (see Figure 1). The uncertainty of the modified models is about ± 5 Wm^{-2} and corresponds to the pyrgeometer measurement uncertainty. The discrepancies of calculated DLR fluxes using the new model and the formula of Prata with respect to the observations are also within the measurement uncertainty. The new model seems to perform slightly better than the empirical formula of Dupont. Moreover, the new model has the advantage that it does not use any additional empirical factors which need to be derived from observations. Thus, no calibration is required as for the empirical schemes.

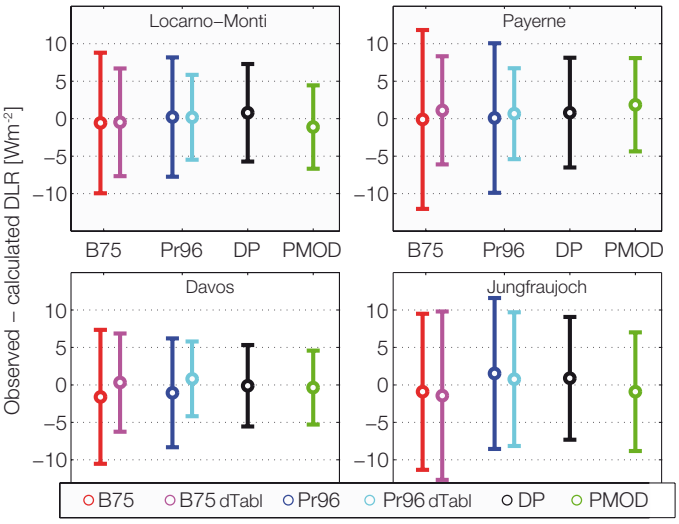

Figure 1. Mean differences (circles) and standard deviation between observed and calculated down-welling long-wave radiation using the models of Brutsaert (B75), Prata (Pr96), Dupont (DP) and the new PMOD model. A lapse rate correction was also applied to the Brutsaert and Prata models (magenta and cyan errorbars, respectively).

References:

Brutsaert W., 1975: On a Derivable Formula for Long-Wave Radiation From Clear Skies, Water. Resour. Res., 11, 742–744.

Dupont J.C., Haeffelin M., Drobinski P., Besnard T.,: 2008, Parametric model to estimate clear-sky longwave irradiance at the surface on the basis of vertical distribution of humidity and temperature, J. Geophys. Res., 113, 7203–7213, doi:10.1029/2007JD009046.

Gröbner J., Wacker S., Vuilleumier L., Kämpfer N.: 2009, Effective atmospheric boundary layer temperature from longwave radiation measurements, J. Geophys. Res., 114(D19116), doi:10.1029/2009JD012274.

Prata A.: 1996, A new long-wave formula for estimating downward clear-sky radiation at the surface, Quarterly Journal of the Royal Meteorological Society, 122, 1127–1151, doi:10.1256/smsqj.53305.

Homogenization of Aerosol Optical Depth Data Sets 1991–2010 in Switzerland

Stephan Nyeki, Christos Halios, Christoph Wehrli, and Julian Gröbner

Various aerosol optical depth (AOD) data sets using automated sun-photometers are available in Switzerland since 1991. Homogenization of these data sets for Davos and the Jungfraujoch is currently proving a challenge. This is not the case for Bern where a decreasing trend in AOD was found.

Measurements of aerosol optical depth (AOD) using sun-photometers at three sites in Switzerland are presented for the 1991–2010 period. Continuous AOD measurements were conducted at Bern (560 m asl; 46.95°N, 7.44°E; Univ. Bern, urban site) using an SPM2000 sun-photometer from 1998–2006, although sporadic measurements exist back to 1992. This site is no longer in operation, but AOD measurements continue at four other sites in Switzerland. AOD time-series from two of these sites are reported here: Davos from 1991–2010 (1580 m asl; 46.82°N, 9.85°E; low-alpine site), and the Jungfraujoch from 1999–2010 (3580 m; 46.55°N, 7.98°E; high-alpine site). Both sites are part of the GAW (Global Atmosphere Watch, WMO) and the Swiss Alpine Climate Radiation Monitoring Network (SACRaM, MeteoSwiss) programs. AOD observations were conducted with the SPM2000 until 2003 and with precision filter radiometers (PFR) from about 1998 onwards.

Sun-photometer measurements from the GAW-PFR network were calibrated against three reference PFRs whose Langley calibrations are traceable to measurements: i) on a balloon gondola, ii) at Mauna Loa (3397 m), and iii) at Izana (2371 m). MeteoSwiss and Univ. Bern calibrations were conducted using the refined Langley method during atmospherically stable conditions. Approximately 5, 16 and 32 exceptionally perfect Langley calibration days per year occurred at Bern, Davos and Jungfraujoch, respectively. AOD was derived according to GAW-PFR procedures (WMO CIMO recommendations). Retrieval errors are estimated to be < 0.010 at λ = 500 nm.

The available AOD time-series at all three sites is shown in Figure 1. Grey curves represent AOD derived with the "SPM-Tool" software package (Ingold et al., 2001), and black curves with the "PFR-Eval" package (Wehrli,). Periods with overlapping AOD at Davos and the Jungfraujoch illustrate the difficulty in homogenizing both data sets. However, a comparison of both sun-photometers using SPMTool at Davos and the Jungfraujoch gave a correlation coefficient > 0.98, indicating that the difference was

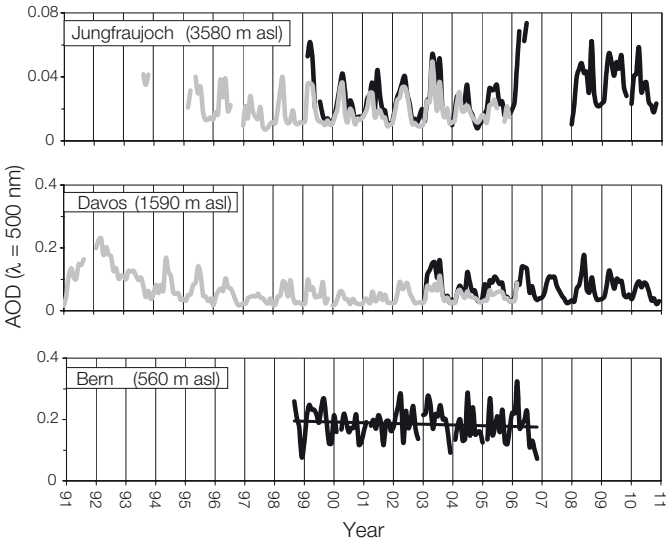

Figure 1. Time-series of monthly AOD averages at: a) Jungfraujoch, b) Davos, and c) Bern. Grey curves represent AOD derived with SPMTool, and black curves with PFR-Eval. The black line indicates a simple linear regression analysis over the measured period.

due to software filters and the cloud-screening algorithms in SPM-Tool and PFR-Eval. Despite these issues, the most notable aspect in Fig.1 is the 1991 Pinatubo volcanic eruption (15°N, 120°E) which resulted in a peak AOD value of ~ 0.20 in Spring 1992 at Davos.

Until the SPM2000 data sets from Davos and the Jungfraujoch are converted for use with PFR-Eval, a trend analysis is restricted to Bern. A simple linear regression analysis indicated a decrease in AOD of about –0.02/decade. A more sophisticated trend analysis is currently being performed.

References: Ingold T., Mätzler C., Kämpfer N., Heimo A.: Aerosol optical depth measurements by means of a sun-photometer network in Switzerland, J. Geophys. Res., 106, 27537–27554, 2001.

Wehrli C.: Remote sensing of Aerosol Optical Depth in a Global surface network, PhD ETH Zürich, No. 17591, 2008. Available at: http://e-collection.ethbib.ethz.ch/view/eth:30693.

A Century of Broadband Atmospheric Transmission over Davos

Daniel Lachat and Christoph Wehrli

We reconstructed a one hundred year record of broadband apparent atmospheric transmission based on pyrheliometer data extracted from the PMOD/WRC archive. The resulting time-series was analyzed for possible decadal trends in atmospheric transmission.

Pyrheliometer measurements at the PMOD were taken between 1909 up to present with various instrumentation on changing scales. It was found that the data coverage is highly varying according to the different measurement regimes at PMOD, when daily observations were replaced by sporadic measurements for calibration purposes. The resulting data was screened against upper and lower limits of solar radiation at given optical airmasses calculated by the SMARTS2-radiative transfer model (Gueymard, 2001). Apparently, no pyrheliometric measurements were taken in the year 1911. The second data gap in the year 1954 arises from yet unsatisfactory homogenization efforts.

As expected, atmospheric transmission at Davos is subject to a pronounced annual cycle as shown in Figure 1. During the winter season, transmission is enhanced due to less aerosol transport as the local sources at lower altitudes are trapped below an inversion layer. We suggest that a possible decadal trend would manifest differently according to the seasonal subsets chosen.

The preliminary results of the calculated transmission-series are displayed in Figure 2. The overlaid cubic trend shows a slight decrease during the 40s and 50s followed by an ongoing increase in transmission starting in the 80s known as Global Dimming and Global Brightening respectively (Ohmura and Wild, 2005). The confidence regions of 2*sigma represent the annual variability mentioned above. Periods of low data coverage result in broader annual variability. The annual cycle presented in Figure 1 will be used to de-seasonalize the transmission-series before a trend analysis will be applied.

The next step will be to evaluate the contribution of aerosols on transmission following the procedure of Gueymard (1998) to retrieve Broadband Aerosol Optical Depth (BAOD). Based on the detrended atmospheric transmission-series, BAOD will be obtained as the residual contribution after subtracting the contributions of air molecules, water vapour and ozone. Therefore, auxiliary data on these components are necessary and have to be quality-screened. The resulting BAOD-series should provide information about the direct effect of aerosols on transmission.

References:

Gueymard C.: Parameterized transmittance model for direct beam and circumsolar spectral irradiance, Solar Energy 71, 325–346, 2001.

Hoyt D., Fröhlich C.: Atmospheric Transmission at Davos 1909–1979, Climate Change 5, 61–71, 1983.

Ohmura A., Wild M.: From dimming to brightening: Decadal changes in surface solar radiation, Science 308, 847–850, 2005.

Gueymard C.: Turbidity Determination from Broadband Irradiance Measurements: A detailed multicoefficient approach, J. of App. Met., 37, 414–435, 1998.

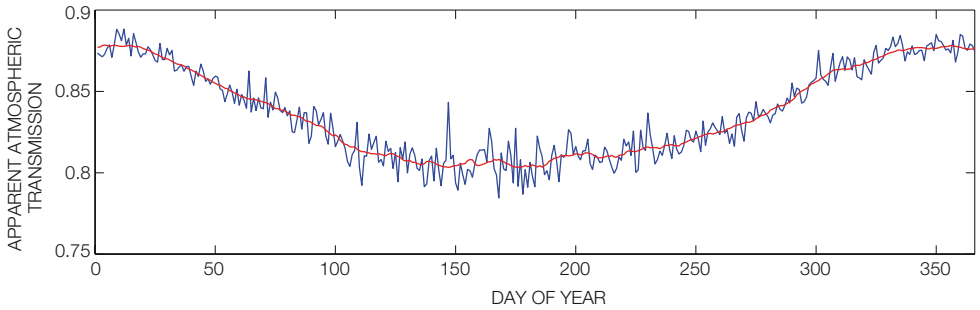

Figure 1. Long-term daily means of atmospheric transmission (solid blue line) with a 20-day running mean (solid red line).

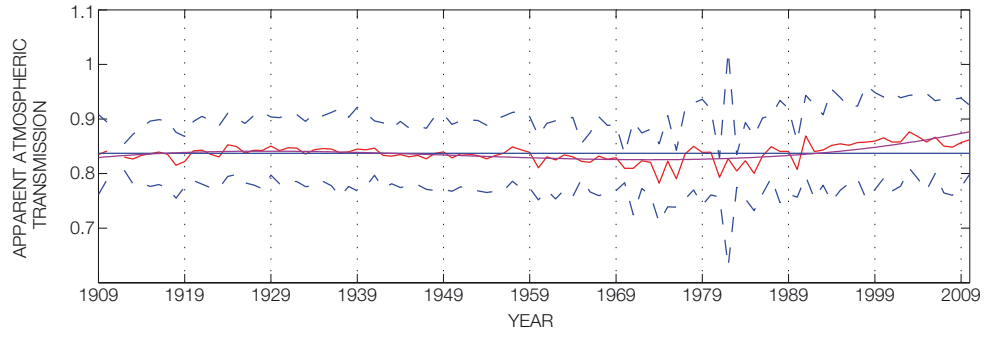

*Figure 2. Annual means of apparent atmospheric transmission (solid red line) overlaid with a cubic trend (solid pink line) and the mean (solid blue line). The 2*sigma-regions (dashed blue lines) represent the annual variablitiy of the specific years.*

A New Approach to Long-Term Reconstruction of the Solar Irradiance

Alexander Shapiro, Werner Schmutz, Eugene Rozanov, Micha Schoell, Margit Haberreiter, Anna Shapiro, and Stephan Nyeki

Evidence showing that the terrestrial climate correlates positively with solar activity has been widely reported. At the same time recent studies suggest very little solar irradiance variability over the last millennia, and hence the mechanism of its impact on climate remains unexplained. We present a new approach to determine centennial variations of the quiet Sun irradiance and show that it leads to a significant increase in the solar irradiance variability. Our findings suggest that solar irradiance variability plays an active role in natural climate change.

We assume that the minimum state of the quiet Sun in time corresponds to the observed quietest area on the present Sun. Then we use available long-term proxies of the solar activity, which are ^{10}Be isotope concentrations in ice cores and 22-year smoothed neutron monitor data, to interpolate between the irradiance of the present quiet Sun and the irradiance of the minimum state of the quiet Sun. This determines the long-term trend in the solar variability which is then superposed with the 11-year activity cycle calculated from the sunspot number. Our approach gives us a direct solar radiative forcing from the present to the Maunder minimum $\Delta F = 1.0 \pm 0.5$ W/m^2 which is significantly larger than the present consensus (about 0.1–0.2 W/m^2). The modulation potentials and the TSI reconstructions are presented in Fig. 1. The difference in the reconstructions allows the error originating from the uncertainties in the proxy data to be estimated (20–50 %, depending on the year). This is large but still significantly less than the change in irradiance between the present and the Maunder minimum.

The magnitude of the solar UV variability, which indirectly affects climate is also found to exceed previous estimates. The effect of enhanced UV variability on the stratosphere is illustrated in Fig. 2. Using a simple 1-D chemistry-climate model by Rozanov et al. (2002) we simulate a much larger change (3–8 times, depending on height) of stratospheric ozone and temperature from 1900 to 2000 driven by increasing solar UV irradiance obtained with our reconstruction compared to that of Lean et al. (2005).

References:

McCracken K.G., McDonald F.B., Beer J., Raisbeck G., Yiou F.: 2004, Journal of Geophysical Research (Space Physics) 109, 12103.

Usoskin I.G., Alanko-Huotari K., Kovaltsov G.A., Mursula K.: 2005, Journal of Geophysical Research (Space Physics) 110, 12108.

Rozanov E. et al.: 2002, From Solar Min to Max: Half a Solar Cycle with SOHO, A. Wilson, ed. (2002) vol. 508 of ESA Special Publication, pp. 181–184.

Lean J., Rottman G., Harder J., Kopp G.: 2005, Sol. Phys. 230, 27.

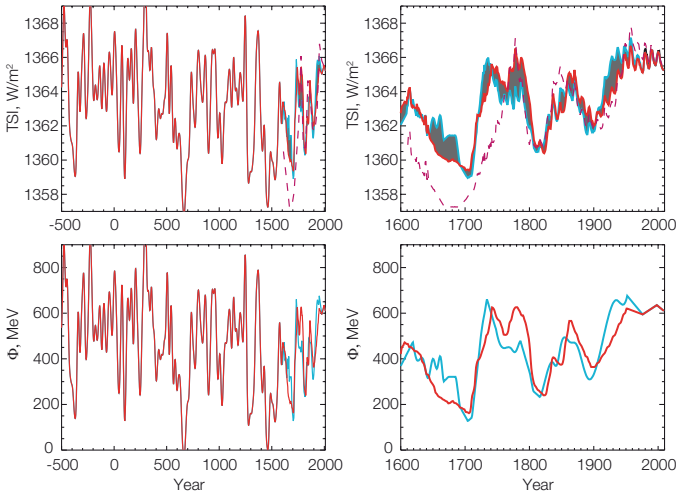

Figure 1. Modulation potential (lower panel) and TSI reconstructions (upper panel) for the last 2500 years. Data prior to 1600 AD are based on the modulation potential derived from ^{10}Be records from the Greenland Ice core Project (red curves). Data since 1600 AD are based on the South Pole and DYE3 ^{10}Be data (red and cyan curves) from McCracken et al. (2004) and neutron monitor data from Usoskin et al. (2005). The grey-shaded area indicates the intrinsic uncertainty. The dashed magenta curve is obtained by using a 22-year average of sunspot number as an activity proxy instead of the modulation potential.

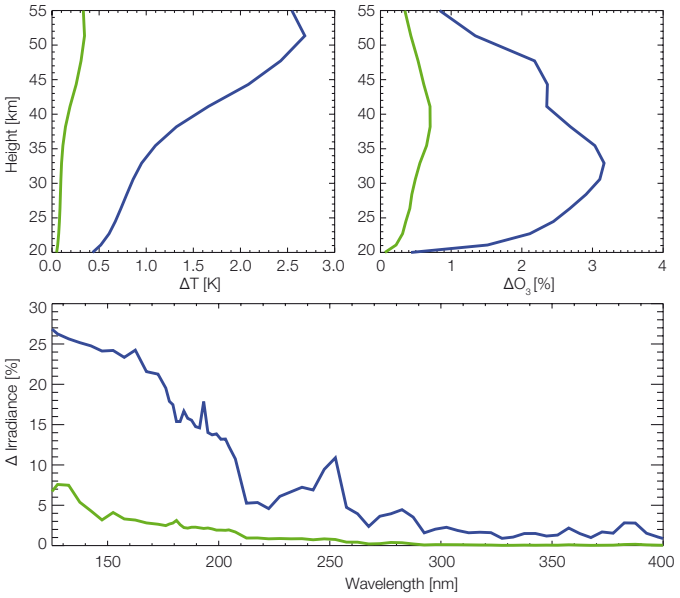

Figure 2. Solar variability and climate response. Changes of 22-year mean spectral solar irradiance (lower panel), stratospheric temperature (upper left panel), and ozone (upper right panel) from 1883–1904 to 1983–2004 obtained from our spectral reconstruction (blue curves) and using the spectral reconstruction of Lean (2005, green curves in above figure).

Modeling the Solar EUV during Quiet Sun Conditions

Margit Haberreiter

We present spectral synthesis calculations of the solar extreme UV (EUV) in spherical symmetry carried out with the 'Solar Modeling in 3D' code. The calculations are based on one-dimensional atmospheric structures that represent a temporal and spatial mean of the chromosphere, transition region, and corona. The synthetic irradiance spectra are compared with the recent calibration spectrum taken with the EUV Variability Experiment onboard the Solar Dynamics Observatory.

The solar EUV irradiance changes on short time-scales of minutes to hours, as well as longer times-scales such as the 27-day solar rotation period and the 11-year solar cycle. Since the peculiarly low 2008 solar minimum there are also indications that the EUV shows a long-term trend.

Incident EUV radiation is absorbed by the Earth's thermosphere, which leads to partial ionization – forming the ionosphere – and a change of its temperature and density. As shown by Solomon et al. (2010) the EUV is in fact the main driver of density changes in the ionosphere. It is understood that the low EUV irradiance during the 2008 minimum phase led to an unprecedented decrease of the ionospheric density (Emmert et al., 2010). Furthermore, as the density of the upper atmosphere has a direct effect on satellite drag (Lilensten et al., 2008) it is clear that models that predict the thermospheric density require improved knowledge of the incident EUV radiation.

Our approach to modeling EUV irradiance variations is to calculate intensity spectra for different features on the solar disk, as identified from various images of the solar disk. Depending on the wavelength range the EUV shows contributions from the chromosphere, transition region (TR), and corona. Therefore, with the code SolMod3D (Haberreiter, 2011) we account for both the optically thick emissions from chromospheric and TR layers, as well as the mainly optically thin emissions from the corona.

The upper panel of Figure 1 shows the EUV spectrum calculated with SolMod3D in high resolution for the quiet Sun compared with the observed spectrum taken with the EVE calibration instrument during a rocket flight on April 14, 2008 (Chamberlin et al., 2009). As the Sun was almost free of any active region on the day of the observation, the spectrum practically represents the quiet Sun.

The synthetic quiet Sun spectrum is derived using a combination of 75 % of the spectrum calculated for the quiet Sun internetwork, 22 % of quiet network, and 3 % of active network. This combination is a typical distribution of features for quiet Sun conditions. The high-resolution spectra show much more detail compared to the observed spectrum. This might be important for understanding the variability in the EUV. In particular, it is to be expected that not all spectral lines vary to the same degree over the solar cycle. Therefore, it is essential to calculate the solar spectrum in full detail. This comparison also shows that it is of great importance to include the complete atomic data for the calculation of the EUV spectrum. The good agreement between the synthetic and observed quiet Sun spectrum shows that the employed atmospheric structures are suitable for irradiance calculations.

References: Chamberlin P.C., Woods T.N., Crotser D.A., Eparvier F.G., Hock R.A., Woodraska D.L.: 2009, Geophys. Res. Lett. 36, L05102.

Emmert J.T., Lean J.L., Picone J.M.: 2010, Geophys. Res. Lett. 37, 12102.

Haberreiter M.: 2011, Solar Physics, in press.

Lilensten J., Dudok deWit T., Kretzschmar M., Amblard P.O., Moussaoui S., Aboudarham J., Auchère F.: 2008, Annales Geophysicae 26, 269.

Solomon S.C., Woods T.N., Didkovsky L.V., Emmert J.T., Qian L.: 2010, Geophys. Res. Lett. 37, 16103.

Acknowledgement: This work has been supported by the Swiss Holcim Stiftung Wissen.

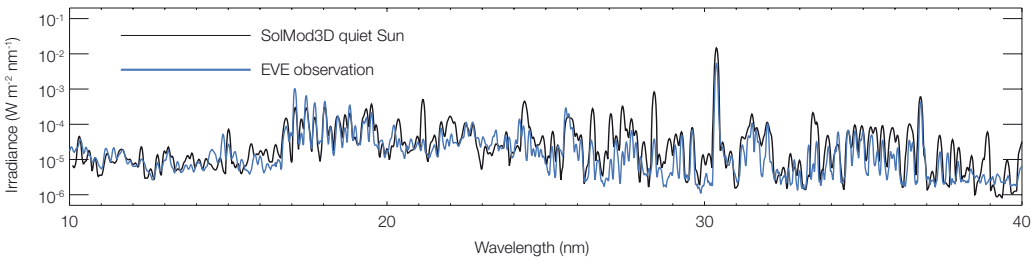

Figure 1. Comparison of the synthetic spectrum calculated with the radiative transfer code SolMod3D. The figure shows the synthetic spectrum (black line) convolved twice with a 1-Å boxcar compared with the EVE rocket spectrum (blue thick line); for details see Haberreiter (2011).

Diagnostics of the Quiet Sun's Magnetism

Alexander Shapiro in collaboration with Institute for Astronomy ETH Zürich, Kiepenheuer-Institut für Sonnenphysik Freiburg i. Br., Istituto Ricerche Solari Locarno

We present a further development of the radiative transfer code POLY. The code is used to interpret the linear polarization signals in CN and C2 absorption lines observed close to the solar limb. This allows us to determine the strength of the turbulent magnetic field of the quiet Sun in the formation regions of CN and C2 absorption lines.

The immense amount of energy stored in magnetic field of the quiet Sun can be a key factor in solving several front-page problems of solar physics, e.g. coupling to the outer atmosphere and the coronal heating. Moreover the evolution of the quiet Sun magnetism could influence the long-term trend in the solar irradiance. Zeeman effect diagnostics fails to measure the magnetic filed of the quiet Sun because of cancellation in circular polarization. However, Hanle effect diagnostics, accessible through the linear polarization spectrum measured close to the solar limb, provides a very sensitive tool for studying the distribution of weak magnetic fields on the Sun.

Recently we developed a numerical scheme to calculate the polarization signal in molecular lines. We used the RH code (Uitenbroek 2001) to solve the statistical equilibrium equations and then iteratively solved the polarized radiative transfer with the POLY code (Fluri et al. 2003, Shapiro 2008).

Here we present an important upgrade of the POLY code. Its original version accounted for the Raman scattering terms in the source function by changing the effective scattering polarizability of the line. In the present version the line source function is properly written as the sum of the scattering integrals, one for each excitation possibility. This allows us to improve the quality of the fit in the CN violet system (Shapiro et al. 2011). The best fit corresponds to magnetic field strengths of 82±10 G (see Fig. 1).

Kleint et al. (2010a, 2010b) initiated the synoptic program to study the evolution of the quiet Sun magnetism with the solar cycle. They concluded that the magnetic field is equally distributed on the Sun during the last solar minimum and that there might be a small modulation of the quiet Sun magnetism between the solar minimum and maximum. The amplitude of this modulation is significantly less than indicated by other proxies of solar activity (e.g. sunspot number or modulation potential). Kleint et al. (2011) used the POLY code to model the polarization signal in C2 lines around 5141 Å. They infer a mean magnetic field strength of 7.4±0.8 G.

References:

Fluri D.M., Nagendra K.N., Frisch H. 2003, A&A 400, 303.

Kleint L., Berdyugina S.V., Shapiro A.I., Bianda M., 2010, A&A 524, A37.

Kleint L., Berdyugina S.V., Gisler D., Shapiro A.I., Bianda M., 2010b, AN 331, 644K.

Kleint L., Shapiro A.I., Berdyugina S.V., Bianda M., 2011, A&A, submitted.

Shapiro A.I., PhD thesis, 2008.

Shapiro A.I., Fluri D.M., Berdyugina S.V., Bianda M., Ramelli, R., 2011, A&A 529, A139.

Uitenbroek H. 2001, ApJ, 557, 389.

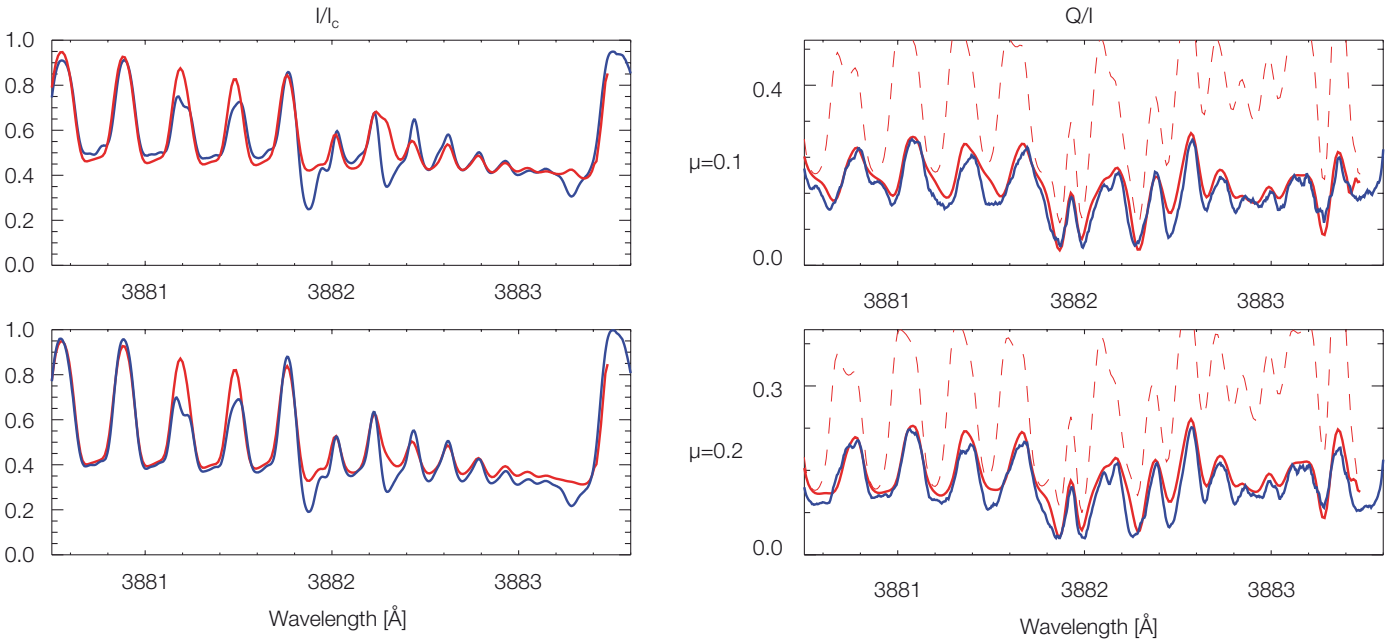

Figure 1. Observations of Stokes I/Ic and Q/I in the region of the (0,0) bandhead and fits obtained with the FALC atmosphere model. The three curves presented in each panel correspond to observations (blue solid) and to the calculations with zero magnetic field (red dashed) and with a magnetic field strength of 82 G (red solid). Note that no differences between the calculated curves are apparent in intensity.

Seismic Signatures of a Second Dynamo Mechanism?

Rosaria Simoniello and Wolfgang Finsterle

We compared the solar cycle related changes in low degree p-mode frequencies from two different experiments, in order to show that the 2-year periodic signal is present in both observations.

The frequencies of the low wave-number solar p-modes are shown to vary with the solar cycle. With increasing solar activity, mode frequencies tend towards higher values.

We quantitatively compared mode frequency-shifts from ground and space-based observations. Long high-quality integrated sunlight observations covering the complete full solar cycle 23 and beginning of solar cycle 24 are provided by the space-based experiment GOLF (Global Oscillation at Low Frequency) on board the ESA/SOHO spacecraft and by the ground-based experiments BiSON (Birmingham Solar Oscillation Network). These observations make possible to determine the solar cycle related changes in p-mode frequencies for low degree modes in the frequency range 2.5 mHz < ν < 4.5 mHz.

Figs. 1–2 show the solar cycle related changes in p-mode frequencies for l=2. We can clearly observe the 11-year periodicity in p-mode frequency variations and a correlation with increasing magnetic activity. This behaviour is opposite to that observed in p-mode amplitudes: with increasing activity p-mode amplitude decreases (Simoniello et al 2010). Furthermore, by looking at the descending phase of solar cycle 23, we can clearly observe a further periodicity of ~2 years. It is also present during the ascending phase, but is less evident.

This mid-term periodicity has been found in Sunspots, Radio Flux and other activity proxies (Belmont et al. 1966, Akioka et al. 1987, Valdès-Galicia et al. 2008, Benevolenskaya et al. 1998). But the acoustic waves reveal another interesting feature: while traces of ~2-year periodicity have been found during the maximum of the activity, acoustic waves show this 2-year periodicity even at the minimum. The end of solar cycle 23 was very peculiar, because it lasted longer than expected, and the Sun was very quiet, reaching lower values in almost all the activity proxies compared to cycle 22. However, acoustic waves still showed some variability during the minimum. This might imply that the Sun was still magnetically active, although no visible manifestations at the surface were present. Further investigations need to be conducted, in order to understand the role played by the second dynamo in solar magnetic activity.

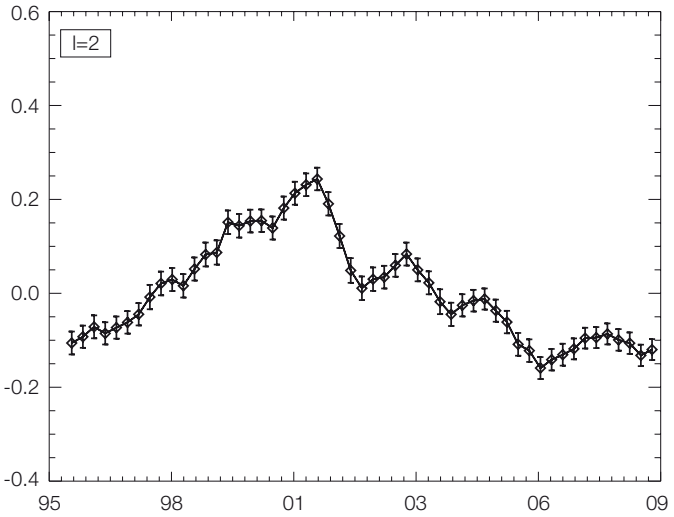

Figure 1. Solar cycle changes in p-mode frequencies from BiSON observations for l=2.

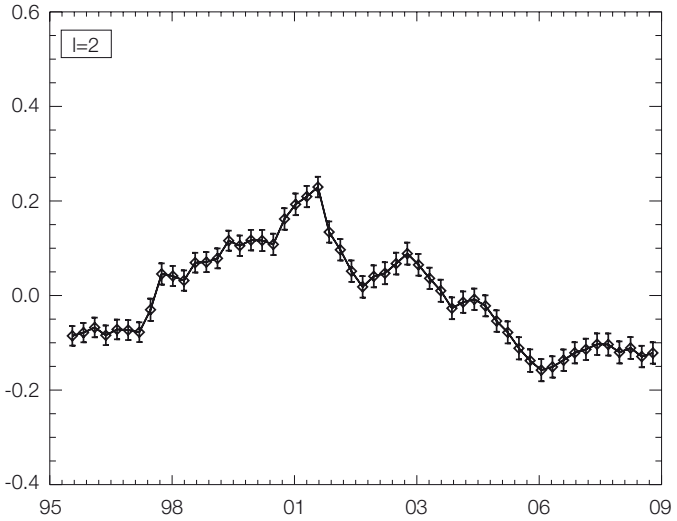

Figure 2. Solar cycle changes in p-mode frequencies from GOLF observations for l=2.

References:

Akioka M., Kubota J., Suzuki M. et al.: 1987, Sol. Phys. 112, 313.

Belmont A.D., Darff D.C., Ultad M.S.: 1966, J. Atmos. Sci. 23, 314.

Benevolenskaya E.E.: 1996, Sol. Phys. 167, 47.

Simoniello R., Finsterle W., Garcia R.A., Salabert S., Jimènez A., Elsworth Y.P., Schunker H.: 2010, A&A 516, A30.

Valdès-Galicia J.F., Velasco V.M.: 2008, AdSpR 41, 297.

Publications

Refereed Publications

Austin J., Scinocca J., Plummer D., Oman L., Waugh D., Akiyoshi H., Bekki S., Braesicke P., Butchart N., Chipperfield M., Cugnet D., Dameris M., Dhomse S., Eyring V., Frith S., Garcia R., Garny H., Gettelman A., Hardiman S., Kinnison D., Lamarque J., Mancini E., Marchand M., Michou M., Morgenstern O., Nakamura T., Pawson S., Pitari G., Pyle J., Rozanov E., Shepherd T., Shibata K., Teyssèdre H., Wilson R., Yamashita Y.: 2010, Decline and recovery of total column ozone using a multimodel time series analysis, J. Geophys. Res., 115, D00M10, doi:10.1029/2010JD013857.

Austin J., Struthers H., Scinocca J., Plummer D.A., Akiyoshi H., Baumgaertner A., Bekki S., Bodeker G., Braesicke P., Brühl C., Butchart N., Chipperfield M., Cugnet D., Dameris M., Dhomse S., Frith S., Garny H., Gettelman A., Hardiman S., Jöckel P., Kinnison D., Kubin A., Lamarque J., Langematz U., Mancini E., Marchand M., Michou M., Morgenstern O., Nakamura T., Nielsen J., Pitari G., Pyle J., Rozanov E., Shepherd T., Shibata K., Smale D., Teyssèdre H., Yamashita Y.: 2010, Chemistry-climate model simulations of spring Antarctic ozone, J. Geophys. Res., 115, D00M11, doi:10.1029/2009JD013577.

Butchart N., Cionni I., Shepherd T., Waugh D., Akiyoshi H., Austin J., Bruehl C., Chipperfield M., Cordero E., Dameris M., Deckert R., Dhomse S., Frith S., Garcia R., Gettelman A., Giorgetta M., Kinnison D., Li F., Mancini E., McLandress C., Pawson S., Pitari G., Plummer D., Rozanov E., Sassi F., Scinocca J., Shibata K., Steil B., Tian W.: 2010, Chemistry-Climate Model Simulations of Twenty-First Century Stratospheric Climate and Circulation Changes, J. Of Climate, 23, 20, 5349–5374.

Charlton-Perez A.J., Hawkins E., Eyring V., Cionni I., Bodeker G.E., Kinnison D.E., Akiyoshi H., Frith S.M., Garcia R., Gettelman A., Lamarque J.F., Nakamura T., Pawson S., Yamashita Y., Bekki S., Braesicke P., Chipperfield M.P., Dhomse S., Marchand M., Mancini E., Morgenstern O., Pitari G., Plummer D., Pyle J.A., Rozanov E., Scinocca J., Shibata K., Shepherd T.G., Tian W., Waugh D.W.: 2010, The potential to narrow uncertainty in projections of stratospheric, ozone over the 21st century, ACP, 10, 19, 9473–9486, doi: 10.5194/acp-10-9473-2010, 2010.

Eyring V., Cionni I., Bodeker G.E., Charlton-Perez A.J., Kinnison D.E., Scinocca J.F., Waugh D.W., Akiyoshi H., Bekki S., Chipperfield M.P., Dameris M., Dhomse S., Frith S.M., Garny H., Gettelman A., Kubin A., Langematz U., Mancini E., Marchand M., Nakamura T., Oman L.D., Pawson S., Pitari G., Plummer D.A., Rozanov E., Shepherd T.G., Shibata K., Tian W., Braesicke P., Hardiman S.C., Lamarque J.F., Morgenstern O., Pyle J.A., Smale D., Yamashita Y.: 2010, Multi-model assessment of stratospheric ozone return dates and ozone recovery in CCMVal-2 models, ACP, 10, 19, 9451–9472, doi: 10.5194/acp-10-9451-2010.

Gerber E.P., Baldwin M.P., Akiyoshi H., Austin J., Bekki S., Braesicke P., Butchart N., Chipperfield M., Dameris M., Dhomse S., Frith S.M., Garcia R.R., Garny H., Gettelman A., Hardiman S.C., Karpechko A., Marchand M., Morgenstern O., Nielsen J.E., Pawson S., Peter T., Plummer D.A., Pyle J.A., Rozanov E., Scinocca J.F., Shepherd T.G., Smale D., Steven C.: 2010, Stratosphere-troposphere coupling and annular mode variability in, chemistry-climate models, JGR, 115, D00M06, doi: 10.1029/2009JD013770.

Gettelman A., Hegglin M., Son S., Kim J., Fujiwara M., Birner T., Kremser S., Rex M., Anel J., Akiyoshi H., Austin J., Bekki S., Braesike P., Bruehl C., Butchart N., Chipperfield M., Dameris M., Dhomse S., Garny H., Hardiman S., Jockel P., Kinnison D., Lamarque J., Mancini E., Marchand M., Michou M., Morgenstern O., Pawson S., Pitari G., Plummer D., Pyle J., Rozanov E., Scinocca J., Shepherd T., Shibata K., Smale D., Teyssedre H., Tian W.: 2010, Multimodel assessment of the upper troposphere and lower stratosphere: Tropics and global trends, JGR, 115, D00M08, doi: 10.1029/2009JD013638.

Gröbner J., Hülsen G., Wuttke S., Schrems O., De Simone S., Gallo V., Rafanneli C., Petkov B., Vitale V., Edvardsen K., Stebel K.: 2009, Quality Assurance of solar UV irradiance in the Arctic, Photochem. Photobiol. Sci., DOI: 10.1039/B9PP00170K.

Haberreiter M., Finsterle W.: 2010, Influence of the Conversion Layer on the Dispersion Relation of Waves in the Solar Atmosphere, Solar Physics, 263, 51–61, doi: 10.1007/s11207-010-9523-6.

Hegglin M., Gettelman A., Hoor P., Krichevsky R., Manney G., Pan L., Son S., Stiller G., Tilmes S., Walker K., Eyring V., Shepherd T., Waugh D., Akiyoshi H., Anel J., Austin J., Baumgaertner A., Bekki S., Braesike P., Bruehl C., Butchart N., Chipperfield M., Dameris M., Dhomse S., Frith S., Garny H., Hardiman S., Jockel P., Kinnison D., Lamarque J., Mancini E., Michou M., Morgenstern O., Nakamura T., Olivie D., Pawson S., Pitari G., Plummer D., Pyle J., Rozanov E., Scinocca J., Shibata K., Smale D., Teyssedre H., Tian W., Yamashita Y.: 2010, Multimodel assessment of the upper troposphere and lower stratosphere: Extratropics, JGR, 115, D00M09, doi: 10.1029/2010JD013884.

Karpechko A., Gillett N., Hassler B., Rosenlof K., Rozanov E.: 2010, Objective assessment of ozone in chemistry-climate model simulations, Atmos. Chem. Phys., 10, 1385–1400.

Refereed Publications

Kazadzis S., Gröbner J., Arola A., Amiridis V.: 2010, The effect of the global UV irradiance measurement accuracy on the single scattering albedo retrieval, Atmos. Meas. Tech., 3, 1029–1037, doi: 10.5194/amt-3-1029-2010.

Kleint L., Berdyugina S.V., Gisler D., Shapiro A.I., Bianda M.: 2010, A synoptic program for large solar telescopes: Cyclic variation of turbulent magnetic fields, Astronomische Nachrichten, 331, 6, 644.

Kleint L., Berdyugina S.V., Shapiro A.I., Bianda M.: 2010, Solar turbulent magnetic fields: surprisingly homogeneous distribution during the solar minimum, Astronomy & Astrophysics, 524 A, 37K.

Kretzschmar M., Dudok de Wit T., Schmutz W., Mekaoui S., Hochedez J.-F., Dewitte S.: 2010, The effect of flares on total solar irradiance, Nature Physics 6, 690–692, doi: 10.1038/nphys1741.

Morgenstern O., Akiyoshi H., Bekki S., Braesicke P., Butchart N., Chipperfield M. P., Cugnet D., Deushi M., Dhomse S.S., Garcia R.R., Gettelman A., Gillett N.P., Hardiman S.C., Jumelet J., Kinnison D.E., Lamarque J.F., Lott F., Marchand M., Michou M., Nakamura T., Olivie D., Peter T., Plummer D., Pyle J.A., Rozanov E., Saint-Martin D., Scinocca J.F., Shibata K., Sigmond M., Smale D., Teyssedre H., Tian W., Voldoire A., Yamashita Y.: 2010, Anthropogenic forcing of the Northern Annular Mode in CCMVal-2 models, JGR, 115, D00M03, doi: 10.1029/2009JD013347.

Morgenstern O., Giorgetta M.A., Shibata K., Eyring V., Waugh D.W., Shepherd T.G., Akiyoshi H., Austin J., Baumgaertner A.J.G., Bekki S., Braesicke P., Bruehl C., Chipperfield M.P., Cugnet D., Dameris M., Dhomse S., Frith S.M., Garny H., Gettelman A., Hardiman S.C., Hegglin M.I., Joeckel P., Kinnison D.E., Lamarque J.F., Mancini E., Manzini E., Marchand M., Michou M., Nakamura T., Nielsen J.E., Olivie D., Pitari G., Plummer D.A., Rozanov E., Scinocca J.F., Smale D., Teyssedre H., Toohey M., Tian W., Yamashita Y.: 2010, Review of the formulation of present-generation stratospheric, chemistry-climate models and associated external forcings, JGR, 115, D00M02, doi: 10.1029/2009JD013728.

Oman L., Plummer D., Waugh D., Austin J., Scinocca J., Douglass A., Salawitch R., Canty T., Akiyoshi H., Bekki S., Braesicke P., Butchart N., Chipperfield M., Cugnet D., Dhomse S., Eyring V., Frith S., Hardiman S., Kinnison D., Lamarque J.F., Mancini E., Marchand M., Michou M., Morgenstern O., Nakamura T., Nielsen J., Olivié D., Pitari G., Pyle J., Rozanov E., Shepherd T., Shibata K., Stolarski R., Teyssèdre H., Tian W., Yamashita Y., Ziemke J.: 2010, Multimodel assessment of the factors driving stratospheric ozone evolution over the 21st century, J. Geophys. Res., 115, D24306, doi:10.1029/2010JD014362.

Ray E., Moore F., Rosenlof K., Davis S., Boenisch H., Morgenstern O., Smale D., Rozanov E., Hegglin M., Pitari G., Mancini E., Braesicke P., Butchart N., Hardiman S., Li F., Shibata K., Plummer D.: 2010, Evidence for changes in stratospheric transport and mixing over the past three decades based on multiple data sets and tropical leaky pipe analysis, J. Geophys. Res., 115, D21304, doi:10.1029/2010JD014206.

Shapiro A.I., Schmutz W., Schoell M., Haberreiter M., Rozanov E.: 2010, NLTE solar irradiance modeling with the COSI code, A&A 517, 48S, doi: 10.1051/0004-6361/200913987.

Skinner S.L., Zhekov S.A., Güdel M., Schmutz W., Sokal K.R.: 2010, X-ray Emission from Nitrogen-Type Wolf-Rayet Stars, AJ 139, 825–838, doi: 10.1088/0004-6256/139/3/825.

Sokal K.R., Skinner S.L., Zhekov S.A., Güdel M., Schmutz W.: 2010, Chandra Detects the Rare Oxygen-type Wolf-Rayet Star WR 142 and OB Stars in Berkeley 87, ApJ 715, 1327–1337, doi: 10.1088/0004-637X/715/2/1327.

Son S.W., Gerber E.P., Perlwitz J., Polvani L.M., Gillett N.P., Seo K.H., Eyring V., Shepherd T.G., Waugh D., Akiyoshi H., Austin J., Baumgaertner A., Bekki S., Braesicke P., Bruhl C., Butchart N., Chipperfield M.P., Cugnet D., Dameris M., Dhomse S., Frith S., Garny H., Garcia R., Hardiman S.C., Jockel P., Lamarque J.F., Mancini E., Marchand M., Michou M., Nakamura T., Morgenstern O., Pitari G., Plummer D.A., Pyle J., Rozanov E., Scinocca J.F., Shibata K., Smale D., Teyssedre H., Tian W., Yamashita Y.: 2010, Impact of stratospheric ozone on Southern Hemisphere circulation change: A multimodel assessment, JGR, 115, D00M07, dpi:10.1029/2010JD014271.

Other Publications

Daglis I.A., Keramitsoglou I., Amiridis V., Petropoulos G., Kourtidis K., Georgoulias A., Melas D., Giannaros T., Sobrino J.A., Manunta P., Gröbner J., Paganini M., Bianchi R.: 2010, Investigating the Urban Heat Island (UHI) Effect in Athens through a Combination of Space, Airborne and Ground-Based Observations. In: 10th COMECAP proceedings, 469–477.

Daglis I.A., Rapsomanikis S., Kourtidis K., Melas D., Papayannis A., Keramitsoglou I., Giannaros T., Amiridis V., Petropoulos G., Sobrino J.A., Manunta P., Gröbner J., Paganini M., Bianchi R.: 2010, Mapping the Urban Heat Island Effect in Athens: Results Obtained from the UHI and Thermopolis 2009 Projects. In: General Assembly EGU, G. Res. Abs., 12, EGU2010-915-1.

Fröhlich C.: 2010, Solar radiometry. In: Observing Photons in Space, M.C.E. Huber, A. Pauluhn, J.L. Culhane, J.G. Timothy, K. Wilhelm, A. Zehnder (eds.), ISSI Scientific Reports Series SR-009, p. 525–540.

Fröhlich C.: 2010, Spectral Solar Irradiance over Solar Cycle 23 from Sunphotometers of VIRGO on SOHO, AGU Fall Meeting 2010, abstract #GC33C-08.

Gröbner J., Hülsen G., Blumthaler M.: 2010, Effect of snow albedo and topography on UV radiation. In: NIWA UV Workshop, 7–9 May 2010, Queenstown.

Haberreiter M., Finsterle W., McIntosh S., Wedemeyer-Böhm S.: 2010, Toward the analysis of waves in the solar atmosphere based on NLTE spectral synthesis from 3D MHD simulations. In: Memorie della Societa Astronomica Italiana, 81, 782.

Hochedez J.-F., Dammasch I., Schmutz W.: 2010, First results from the LYRA solar UV radiometer. In: 38th COSPAR Scientific Assembly, COSPAR, Plenary Meeting 38, p. 1090.

Kleint L., Berdyugina S.V., Shapiro A.I., Bianda M.: 2010, Turbulent Magnetic Fields in the Quiet Sun: A Search for Cyclic Variations. In: SOHO-23: Understanding a Peculiar Solar Minimum, ASP Conference Series, 428, 103.

Lamy P., Vives S., Curdt W., Dame L., Davila J., Defise J.M., Fineschi S., Heinzel P., Kuzin S., Schmutz W., Tsinganos K., Turck-Chièze S., Zhukov A.: 2010, Towards a New Formation Flying Solar Coronagraph. In: K. Tsinganos, D. Hatzidimitriou, T. Matsakos (eds.), Advances in Hellenic Astronomy during the IYA09, ASP Conf. Ser. Vol. 424, p. 15–18.

Lamy P., Damé L., Curdt W., Davila J., Defise J.M., Fineschi S., Heinzel P., Howard R., Kuzin S., Schmutz W., Tsinganos K., Turck-Chièze S., Zhukov A.: 2010, ASPIICS / PROBA-3: A formation flying externally-occulted giant coronagraph mission. In: 38th COSPAR Scientific Assembly, COSPAR, Plenary Meeting 38, p. 2858.

Melo S.M.L., Thuillier G., Claudel J., Haberreiter M., Mein N., Schmutz W., Shapiro A., Sofia S., Short C.I.: 2010, Model studies of the solar limb shape variation with wavelength within the PICARD project. In: 38th COSPAR Scientific Assembly, COSPAR, Plenary Meeting 38, p. 1756.

Nyeki S., Wehrli C.: 2010, Long-term aerosol optical depth measurements at the Jungfraujoch. In: Symposium on Atmospheric Chemistry and Physics at Mountain Sites, scnat, Interlaken, Switzerland.

Quesnel A., Dennis B.R., Fleck B., Fröhlich C., Hudson H.S., Tolbert A.K.: 2010, The Signature of Flares in VIRGO Total Solar Irradiance Measurements. In: SOHO-23: Understanding a Peculiar Solar Minimum, S.R. Cranmer, J.T. Hoeksema, J.L. Kohl (eds.). ASP Conf. Ser. 428, 133–136.

Rozanov E., Dorf D., Arfeuille F., Brönnimann S., Calisto M., Egorova T., Fischer A., Heckendorn P., Luo B.-P., Peter T., Rozanov E., Shapiro A.V., Schmutz W., Schraner M., Stenke A., Zubov V.: 2010, Effects of the solar spectral irradiance changes during the first half of 20th century on chemistry and climate. In: 38th COSPAR Scientific Assembly, COSPAR, Plenary Meeting 38, p. 21.

Rozanov E., Egorova T., Shapiro A., Shapiro A., Schmutz W.: 2010, Modeling the impact of the solar UV irradiance on the middle atmosphere. In: 38th COSPAR Scientific Assembly, COSPAR, Plenary Meeting 38, p. 1103.

Schmutz W., Fehlmann A., Finsterle W., Rozanov E.: 2010, Total Solar Irradiance: Present status of TSI observations. In: 38th COSPAR Scientific Assembly, COSPAR, Plenary Meeting 38, p. 1689.

Shapiro A., Rozanov E., Shapiro A., Egorova T., Schmutz W., Peter T.: 2010, Response of the middle atmosphere to short-term solar irradiance variability during different Quasi-Biennial Oscillation phases. In: 38th COSPAR Scientific Assembly, COSPAR, Plenary Meeting 38, p. 138.

Other Publications

Shapiro A., Schmutz W., Thuillier G., Schoell M., Haberreiter M., Rozanov E.: 2010, Modeling of the current TSI and SSI and its reconstruction to the past. In: 38th COSPAR Scientific Assembly, COSPAR, Plenary Meeting 38, p. 134.

Shapiro A., Schmutz W.K., Thuillier G., Rozanov E., Haberreiter M., Schoell M., Shapiro A., Nyeki S.: 2010, New SSI and TSI reconstruction suggests large value of the radiative solar forcing, AGU Fall Meeting 2010, abstract #GC21B-0875.

Skinner S.L., Sokal K.R., Zhekov S.A., Güdel M., Schmutz W.: 2010, Chandra X-ray Observations of the Young Stellar Cluster Berkeley 87 and its Oxygen-type Wolf-Rayet Star WR 142, AAS Meeting #215, BAAS Vol. 41, p. 567.

Thuillier G., Bolsee D., Schmidtke G., Schmutz W., Shapiro A., Nikutowski B.: 2010, The Absolute Solar Irradiance Spectrum at Solar Minimum Activity Measured by the SOLSPEC and SOL-ACES Spectrometers from 17 to 3000 nm Placed on Board the International Space Station. In: 38th COSPAR Scientific Assembly, COSPAR, Plenary Meeting 38, p. 17.

Thuillier G., Schmutz W., Dewitte S.: 2010, The PICARD Mission: an investigation based on measurements dedicated to solar and climate modeling. In: 38th COSPAR Scientific Assembly, COSPAR, Plenary Meeting 38, p. 1094.

Wilhelm K., Fröhlich C.: 2010, Photons – from source to detector. In: Observing Photons in Space, M.C.E. Huber, A. Pauluhn, J.L. Culhane, J.G. Timothy, K. Wilhelm, A. Zehnder (eds.). ISSI Scientific Reports Series SR-009, p. 23–54.

Administration

Personnel Department

Sonja Degli Esposti

In 2010, five new employees were hired. In August, Andreas Schätti filled the vacancy in our workshop for the development of our commercial instruments. Also in August, Thierry Hartmann joined the electronics department as a new apprentice.

A few months later, in October, Markus Suter started his PhD Thesis within the project "Experimental Characterization of a new Absolute Radiometer for SI-traceable Solar Irradiance Measurements". Markus is well-known at PMOD/WRC due to several stints as a civilian conscript during the last years. We are happy to have him in our team again.

The electronics department gained another member. Etienne de Coulon is a software development engineer, and supports our Solar Spectroradiometer Project. Bienvenue Etienne!

Samuel Prochazka, electronics technician, left our institute after more than four years and started his military service.

The continuously increasing number of calibration services induced us to strengthen the administration team: Irene Keller joined the PMOD/WRC just after the IPC XI and is in charge of import/export shipment at our institute.

At the end of March, Uwe Schlifkowitz, PhD student, left our institute.

By the end of the year, our two cleaners and housekeepers, Denise Dicht and Jutta Jäger left the institute. We thank both of them for their dedication and for looking after our welfare. Stana Petrovic took over their position and began in November.

Last but not least – Silvio Koller, head of the electronics department, left our institute after eight years. Silvio started a new career as managing director in a solar energy company. He was closely involved in the management of our latest space experiments and in his role as head of the electronics department, responsible for many small and large projects at our institute. Silvio was a respected head and an appreciated colleague. We all thank him for his commitment towards our institute and wish him happiness and success in his new job.

Manfred Gyo took over the position as head technical department on 1st January, 2011.

As in every year – numerous civilian service conscripts supported our work. Many thanks again to them all.

Scientific Personnel

Prof. Dr. Werner Schmutz	Director, physicist
Dr. Tatiana Egorova	Climate group scientist, meteorologist
Dr. Wolfgang Finsterle	Head WRC-section solar radiometry, physicist
Dr. Claus Fröhlich	PI VIRGO, physicist (retired)
Dr. Julian Gröbner	Head WRC-sections IR radiometry, WORCC, and EUVC, physicist
Dr. Margit Haberreiter	Scientist, physicist
Dr. Gregor Hülsen	EUVC scientist, physicist
Dr. Piotr Kiedron	Visiting scientist, physicist (until 31.1.2011)
Dr. Stephan Nyeki	WORCC scientist, physicist
Dr. Eugene Rozanov	Climate group scientist, physicist
Dr. Alexander Shapiro	Postdoc solar physics group, physicist
Dr. Rosaria Simoniello	Postdoc solar physics group, physicist
Markus Suter	Scientist, project DARA
	PhD Student, UNIZH (since 1.11.2010)
Dr. Christoph Wehrli	WORCC scientist, physicist
André Fehlmann	PhD student, UNIZH
Daniel Lachat	PhD student, UNIBE
Uwe Schlifkowitz	PhD student, University Freiburg i. B. (until 31.3.2010)
Edgar Schmucki	PhD student, UNIBE (since 01.05.2010)
Micha Schöll	PhD student, ETHZ
Anna Shapiro	PhD student, ETHZ
Stefan Wacker	PhD student, UNIBE
Mathias Hauser	Internship, ETHZ (30.8. until 12.11.2010)

Technical Personnel

Silvio Koller	Head technical department, electronic engineer, Quality System manager (until 31.12.2010)
Manfred Gyo	Head technical department, electronic engineer, Quality System manager (since 01.01.2011)
Daniel Bühlmann	Technician
Etienne de Coulon	Software development engineer (since 01.11.2010)
Daniel Pfiffner	Project manager space experiments, deputy head technical department and Quality System, electronic engineer
Andreas Schätti	Mechanician (since 1.8.2010)
Marco Senft	Software developer
Ricco Soder	Development engineer
Marcel Spescha	Technician
Christian Thomann	Technician
Diego Wasser	Electronic technician
Matthias Müller	Electronics apprentice, 2nd year
Samuel Prochazka	Electronics apprentice, 4th year Electronic technician (until 31.10.2010)
Thierry Hartmann	Electronics apprentice, 1st year (since 1.8.2010)

Administration

Sonja Degli Esposti	Head administration/Human Resources
Stephanie Ebert	Administration, book-keeping
Irene Keller	Administration, import/export (since 20.10.2010)
Nadia Casanova	Administration apprentice, 2nd/3rd year

Caretaker

Denise Dicht	General caretaker, cleaning (until 30.11.2010)
Regula Dicht	Cleaning, part time
Jutta Jäger	Cleaning, part time (until 31.12.2010)
Stana Petrovic	General caretaker, cleaning (since 15.11.2010)

Civilian Service Conscripts

Roman Koller	16.04.2010
Daniel Würsch	until 12.02.2010
Andreas Städler	19.04.–18.06.2010
Reto Bloch	15.02.–09.04.2010
Jan Grünenfelder	31.05.–27.08.2010
Damian Manser	14.06.–07.09.2010
Claudio Dellagiacoma	30.08.–29.10.2010
Ivan Frollano	13.09.–15.10.2010
Andreas Elmer	since 18.10.2010
Detlef Conradin	since 01.11.2010

Public Semninars

25/02/2010	Edgar Schmucki, Global Dimming and Brightening in IPCC-GCM models	06/07/2010	Axel Kreuter, University Innsbruck, Austria, Polarised Sky Radiance Imaging
03/03/2010	Julien Anet, Atmospheric pollution modeling: Coupling COSMO-CLM [Land dynamics] to COSMO-ART [Chemical]	24/08/2010	Friedhelm Steinhilber, EAWAG, What can cosmogenic radionuclides tell about solar activity and what not?
03/05/2010	Prof. Siddhartha, ETH Zurich, High-resolution well-balanced schemes for simulating waves in the solar atmosphere	03/09/2010	Christos Halios, University Athens, Greece, Indoor Air Quality in a densely populated city (Athens, Greece)

Course of Lectures, Participation in Commissions

Werner Schmutz	Course of lecture *Astronomie*, HS 2010, ETH-ZH Examination expert in astronomy, BSc ETH-ZH Vice-president of the International Radiation Commission (IRS, IAMAS) Comité consultatif de photométrie et radiométrie (CCPR, OICM WMO) Swiss representative in the Committee on Space Research (COSPAR) President of the national Committee on Space Research, Commission of SCNAT Executive board of the Swiss Society Astronomy Astrophysics (SSAA), SCNAT GAW-CH working group (MeteoSwiss) Swiss Management Committee delegate to the COST action ES0803 (ECF)
Wolfgang Finsterle	CIMO expert team on Standardization
Julian Gröbner	Course of Lecture *Solar Ultraviolet Radiation* HS 2010, ETH-ZH GAW-CH Working group (MeteoSwiss) NEWRAD Scientific committee Chairman of Infrared Working group of Baseline Surface Radiation Network (BSRN) International Radiation Commission (IRS, IAMAS) CIMO expert team on New In-Situ Technologies
Margit Haberreiter	Course of lecture *Astronomie,* HS 2010, ETH-ZH, 2 lectures Scientific Organizing Committee of the IAU Symposium 286
Eugene Rozanov	International Commission on the Middle Atmosphere (ICMA, IAMAS)
Christoph Wehrli	GAW-CH Working group (MeteoSwiss) Scientific Advisory Group Aerosol (WMO/GAW) SAG sub group AOD, chairman (WMO/GAW) Working group Baseline Surface Radiation Network (WMO/WCRP)

Donations

A long-time loyal donor to PMOD/WRC, Mr. Daniel Karbacher from Küsnacht, ZH, has made an extra investment possible in addition to those covered by the regular budget. Through his generous contribution we were able to purchase a fast computer module including a large and fast storage in 2010. This dedicated investment makes long-term climate simulations possible, which need months of computing time. For many computations it is an advantage to rely on a dedicated “normal” computer which is in-house. Our climate program SOCOL runs considerably faster on computer clusters which allow parallel computing.

However, because computing time on computer clusters has to be shared with other users, computation on such facilities is often considerably delayed. Therefore, it turns out that at times of high demand on a computer cluster, the real time that has elapsed for the user until the computation is available, is longer on a computer cluster than for a dedicated normal computer which is always 100 % available. We can now conduct extended runs in-house, and also have time on computer clusters such as Brutus belonging to the ETH Zürich. Having both options available is a clear advantage.

Modernization and Renovation of the Institute Building

Werner Schmutz

The construction of the emergency exit stairwell that began in 2009 was finished in the first half of last year. In addition to the amount listed in the 2009 annual report, there was an additional expenditure of CHF 199'000.00 which included an upgrade of the heating system in the mechanical workshop.

Construction equipment was installed in autumn, just after the end of IPC XI, for the main phase of the PMOD/WRC renovation project. A building-crane and container offices for the construction workers in front of the building used up half the car park space. Technical department staff will remain at the PMOD/WRC site during the whole construction period. A provisional two-storey building was put together with nine containers, serving as offices and workshops. Measurement instruments that were previously installed on the Old Schoolhouse roof were installed on the container roofs. The pictures give an impression of the changing surroundings and working conditions at the PMOD/WRC.

Figure 1. The north side, i.e. the entrance from the car park, of the provisional technical department.

Figure 2. The building crane in the background appears to sit behind the World Standard Group (WSG) in the lower left-hand corner. The WSG is kept running despite the start of construction work in the basement and at the back of the Old Schoolhouse.

Figure 3. Students from the Schweizerische Alpine Mittelschule Davos helped to empty the packed PMOD attic during their winter break.

Bilanz 2010 inklusive Drittmittel

Aktiven	31.12.2010 CHF
Flüssige Mittel/Wertschriften	1'301'422.55
Forderungen	234'564.95
Aktive Rechnungsabgrenzungen	234'405.19
	1'770'392.69
Passiven	
Verbindlichkeiten	147'284.40
Kontokorrent Stiftung	35'566.05
Passive Rechnungsabgrenzungen	427'705.74
Rückstellungen	960'695.19
Eigenkapital	199'141.31
	1'770'392.69

Erfolgsrechnung 2010 inklusive Drittmittel

	CHF
Ertrag	
Beitrag Bund Betrieb WRC	1'287'868.00
Beitrag Kanton Graubünden	214'601.00
Beitrag Gemeinde Davos	555'470.00
Beitrag Gemeinde Davos, Mieterlass	149'486.60
Beitrag Bund (BBL) Bau Fluchttreppe/Lift	185'020.00
Beitrag Bund (BBL) Vorprojekt Umbau Institutsgebäude	865'000.00
Beitrag GAW/CH für EUVC	164'190.00
Forschungsbeitrag EUSAAR	24'114.40
Indirekte Kosten SOTERIA	40'276.30
Overhead SNF	23'381.00
Instrumentenverkäufe	339'523.50
Kalibrationen	236'714.80
Übriger Ertrag	35'871.22
Finanzertrag	17'163.05
Ausserordentlicher Ertrag	2'676.61
Auflösung Rückstellungen	168'416.20
Drittmittel	1'148'164.45
	5'457'937.13

	CHF
Aufwand	
Personalaufwand	3'095'464.45
Investitionen	344'513.49
Unterhalt	38'987.11
Verbrauchsmaterial	204'215.73
Verbrauch Commercial	191'106.67
Reisen, Kongresse, Kurse	154'347.98
Raumaufwand/Energieaufwand	220'610.55
Verwaltungsaufwand	88'019.45
Finanzaufwand	13'723.24
Übriger Betriebsaufwand	34'487.74
BBL, Bau Fluchttreppe/Lift	185'020.00
BBL, Vorprojekt Umbau Institutsgebäude	865'000.00
	5'435'496.41
Ergebnis 2010	22'440.72
	5'457'937.13

Abbreviations

AERONET	Aerosol Robotic Network, GSFC
AOD	Aerosol Optical Depth
ASRB	Alpine Surface Radiation Budget
BIPM	Bureau International des Poids et Mesures, Paris, F
BISON	Birmingham Solar Oscillation Network
BOLD	Blind to Optical Light Detector
BOS	Bolometric Sensor, Belgium instrument on the mission PICARD
BSRN	Baseline Surface Radiation Network of the WCRP
BUSOC	Belgian User Support and Operation Centre of ESA
CCM	Chemistry-Climate Model
CAS	Commission for Atmospheric Sciences, Commission of WMO
CCPR	Comité Consultatif de Photométrie et Radiométrie, BIPM
CIE	Commission Internationale de l'Eclairage
CIPM	Comité International des Poids et Mesures
CIMO	Commission for Instruments and Methods of Observation of WMO, Geneva
CMC	Calibration and Measurement Capabilities
CNES	Centre National d'Etudes Spatiales, Paris, F
CNRS	Centre National de la Recherche Scientifique, Service d`Aéronomie Paris
CoI	Co-Investigator of an Experiment/Instrument/Project
COSI	Code for Solar Irradiance – Solar Atmosphere Radiation Transport Code developed at PMOD/WRC
COSPAR	Commission of Space Application and Research of ICSU, Paris, F
CSAR	Cyrogenic Solar Absolute Radiometer
CTM	Chemical Transport Model
CUCF	Central UV Calibration Facility, NOAA, Boulder, USA
DIARAD	Dual Irradiance Absolute Radiometer of IRMB
DLR	Deutsche Luft und Raumfahrt
ESA	European Space Agency
ESF	European Science Foundation
ESTEC	European Space Research and Technology Center, Noordwijk, NL
ETH	Eidgenössische Technische Hochschule (Z: Zürich, L: Lausanne)
EURECA	European Retrievable Carrier, flown August 1992–June 1993 with SOVA Experiment of PMOD/WRC
EUSAAR	FP6 project: European Supersites for Atmospheric Aerosol Research
EUV	Extreme Ultraviolet Radiation
EUVC	European Ultraviolet Calibration Center at PMOD/WRC
FMI	Finnish Meteorological Institute
FP7	European Framework Program of the European Commission
FRC-III	Third Filter Radiometer Comparison
GAW	Global Atmosphere Watch, an Observational Program of WMO
GAWTEX	GAW Training & Education Center
GCM	General Circulation Model
GHG	Greenhouse Gases
GOLF	Global Oscillations at Low Frequencies, Experiment on SOHO
GSFC	Goddard Space Flight Center, Greenbelt, MD, USA
IACETH	Institute for Climate Research of the ETHZ
IAMAS	International Association of Meteorology and Atmospheric Sciences of IUGG
IAU	International Astronomical Union of ICSU, Paris, F
ICSU	International Council of Scientific Unions, Paris, F
IPC	International Pyrheliometer Comparisons
IR	Infrared
IRC	International Radiation Commission, Commission of IAMAS
IRIS	Infrared Integrating Sphere Radiometer
IRMB	Institut Royal Météorologique de Belgique, Brussel, B
IRS	International Radiation Symposium of the Radiation Commission of IAMAS
IRSOL	Istituto Ricerche Solari Locarno
ISO/IEC	International Oranisation for Standardization/International Electrotechnical Commission
ISS	International Space Station
IUGG	International Union of Geodesy and Geophysics of ISCU
JRC	Joint Research Center of the European Commission in Ispra, I
KIS	Kiepenheuer-Institut für Sonnenphysik, Freiburg i.Br., D
LATMOS	Laboratoire Atmosphères, Milieux, Observations Spatiales, French research institution
LYRA	Lyman-alpha Radiometer, Experiment on PROBA 2, built by PMOD/WRC
METAS	Federal Office of Metrology
MGO	Main Geophysical Observatory, St. Petersburg, RUS
MITRA	Monitor to Determine the Integrated Transmittance
NASA	National Aeronautics and Space Administration, Washington DC, USA
NEWRAD	New Developments and Applications in Optical Radiometry
NILU	Norwegian Institute for Air Research
NIST	National Institute of Standards and Technology, Gaithersburg, MD, USA
NOAA	National Oceanographic and Atmospheric Administration, Washington DC, USA
NPL	National Physical Laboratory, Teddington, UK
NRL	Naval Research Laboratory, Washington DC, USA
NREL	National Renewable Energy Lab, Golden, CO, USA
ODS	Ozone Destroying Substances
PFR	Precision Filter Radiometer
PI	Principle Investigator, Leader of an Experiment/Instrument/Project
PICARD	French Space Experiment to Measure the Solar Diameter, to be launched 2010
PMOD	Physikalisch-Meteorologisches Observatorium Davos
PMO6	PMO6 Type Radiometer
PREMOS	Precision Monitoring of Solar Variability, PMOD/WRC Experiment on PICARD, to be launched 2010
PROBA 2	ESA Technology Demonstration Space Mission, launched 2 December 2009
PRODEX	Program for the Development of Experiments, ESA
PTB	Physikalisch-Technische Bundesanstalt, Braunschweig & Berlin, D
ROB	Royal Observatory of Belgium
QASUME	Quality Assurance of Spectral Ultraviolet Measurements in Europe
QMS	Quality Management System
RA	Regional Association of WMO
SCNAT	Swiss Academy of Sciences
SCOPES	Scientific Collaboration between Eastern Europe and Switzerland, Grant of the SNSF
SLF	Schnee und Lawinenforschungsinstitut, Davos
SFI	Schweiz. Forschungsinstitut für Hochgebirgsklima und Medizin, Davos
SI	International System of Units
SIAF	Schweiz. Institut für Allergie- und Asthma-Forschung, Davos
SMHI	Swedish Meteorological and Hydrological Institute
SNSF	Swiss National Science Foundation
SOCOL	Combined GCM and CTM Computer Model, developed at PMOD/WRC
SOHO	Solar and Heliospheric Observatory, Space Mission of ESA/NASA
SOLAR	Experiment Platform on the ISS
SORCE	Space Mission of NASA
SOTERIA	Solar-Terrestrial Investigations and Archives
SOVA	Solar Variability Experiment on EURECA
SOVIM	Solar Variability and Irradiance Monitoring, PMOD/WRC Experiment on the International Space Station Alpha, 2008
STEP	Solar Terrestrial Energy Program of SCOSTEP/ICSU
SUSIM	Solar Ultraviolet Spectral Irradiance Monitor on Board UARS
UARS	Upper Atmosphere Research Satellite of NASA
UV	Ultraviolet
UVA	UV Radiation in the Range of 315–400 nm
UVB	UV Radiation in the Range of 280–315 nm
VIRGO	Variability of Solar Irradiance and Gravity Oscillations, PMOD/WRC Experiment on SOHO, launched December 1995
WCRP	World Climate Research Program
WDCA	World Data Center for Aerosols, Ispra, I
WIGOS	WMO Integrated Global Observing System
WIS	WMO Information System
WISG	World Infrared Standard Group of Pyrgeometer, maintained by WRC
WMO	World Meteorological Organization, a United Nations Specialized Agency, Geneva
WRC	World Radiation Center, Davos
WRC-IRS	Infrared Radiometry Section of WRC
WRC-SRS	Solar Radiometry Section of WRC
WRC-WORCC	World Optical Depth Research and Calibration Center, WRC Section
WRDC	World Radiation Data Center, St. Petersburg, RUS
WRR	World Radiometric Reference
WSG	World Standard Group, realizing the WRR, maintained by WRC
WWW	World Weather Watch, an Observational Program of WMO

Annual Report 2010

Editors: Stephanie Ebert and Werner Schmutz
Publication by PMOD/WRC

Edition: 650, printed 2011

PMOD/WRC, Davos, Switzerland

Dorfstrasse 33, 7260 Davos Dorf, Switzerland
Phone +41 81 417 51 11, Fax +41 81 417 51 00
www.pmodwrc.ch